HHS Public Access

Author manuscript

Neurobiol Dis. Author manuscript; available in PMC 2017 January 05.

Published in final edited form as:

Neurobiol Dis. 2017 January ; 97(Pt A): 46–59. doi:10.1016/j.nbd.2016.10.006.

The sigma-1 receptor mediates the beneficial effects of pridopidine in a mouse model of Huntington disease

Daniel Ryskamp[a], **Jun Wu**[a], **Michal Geva**[b], **Rebecca Kusko**[c], **Iris Grossman**[b], **Michael Hayden**[b,*], and **Ilya Bezprozvanny**[a,**]

[a]Department of Physiology, University of Texas Southwestern Medical Center, Dallas, TX 75390, USA

[b]Teva Pharmaceutical Industries, 5 Basel St., Petach Tikva 49131, Israel

[c]Immuneering Corporation, Cambridge, MA 02142, USA

Abstract

The tri-nucleotide repeat expansion underlying Huntington disease (HD) results in corticostriatal synaptic dysfunction and subsequent neurodegeneration of striatal medium spiny neurons (MSNs). HD is a devastating autosomal dominant disease with no disease-modifying treatments. Pridopidine, a postulated “dopamine stabilizer”, has been shown to improve motor symptoms in clinical trials of HD. However, the target(s) and mechanism of action of pridopidine remain to be fully elucidated. As binding studies identified sigma-1 receptor (S1R) as a high-affinity receptor for pridopidine, we evaluated the relevance of S1R as a therapeutic target of pridopidine in HD. S1R is an endoplasmic reticulum - (ER) resident transmembrane protein and is regulated by ER calcium homeostasis, which is perturbed in HD. Consistent with ER calcium dysregulation, we observed striatal upregulation of S1R in aged YAC128 transgenic HD mice and HD patients. We previously demonstrated that dendritic MSN spines are lost in aged corticostriatal co-cultures from YAC128 mice. We report here that pridopidine and the chemically similar S1R agonist 3-PPP prevent MSN spine loss in aging YAC128 co-cultures. Spine protection was blocked by neuronal deletion of S1R. Pridopidine treatment suppressed supranormal ER Ca^{2+} release, restored ER calcium levels and reduced excessive store-operated calcium (SOC) entry in spines, which may account for its synaptoprotective effects. Normalization of ER Ca^{2+} levels by pridopidine was prevented by S1R deletion. To evaluate long-term effects of pridopidine, we analyzed expression profiles of calcium signaling genes. Pridopidine elevated striatal expression of calbindin and homer1a, whereas their striatal expression was reduced in aged Q175KI and YAC128 HD mouse models compared to WT. Pridopidine and 3-PPP are proposed to prevent calcium dysregulation and synaptic loss in a YAC128 corticostriatal co-culture model of HD. The actions of pridopidine

*Correspondence to: M. Hayden, 5 Basel St., Petach Tikva 49131, Israel. **Correspondence to: I. Bezprozvanny, 5323 Harry Hines Blvd., ND12.200, Dallas, TX 75390, USA.

Competing interests

The remaining authors declare no competing financial interests.

No non-financial conflicts of interest exist for any of the authors.

Authors' contributions

DR and JW carried out studies with primary neuronal cultures and Western blotting analysis. MG, RK, IG analyzed gene expression data. MH, IB – designed and conceived the study and participated in its design and coordination. DR, IB – drafted the manuscript, MG, RK, IG, MH – helped to revise the manuscript. All authors read and approved the final manuscript.

were mediated by S1R and led to normalization of ER Ca^{2+} release, ER Ca^{2+} levels and spine SOC entry in YAC128 MSNs. This is a new potential mechanism of action for pridopidine, highlighting S1R as a potential target for HD therapy. Upregulation of striatal proteins that regulate calcium, including calbindin and homer1a, upon chronic therapy with pridopidine, may further contribute to long-term beneficial effects of pridopidine in HD.

Keywords

Huntington disease; Pridopidine; 3-PPP; Sigma-1 receptor; Medium spiny neurons; YAC128 mice; Corticostriatal co-culture; Synaptic instability; Store-operated calcium entry

1. Introduction

Huntington disease (HD) is a progressive neurodegenerative disease resulting from a dominantly-inherited trinucleotide (CAG) repeat expansion in the huntingtin gene, encoding polyglutamine-expanded mutant Huntingtin (mHtt) protein (MacDonald et al., 1993). HD symptoms, which include motor, cognitive and psychiatric disturbances, typically present around 40 years of age and progressively worsen until death approximately 20 years after diagnosis (Foroud et al., 1999). HD management is limited to supportive care and symptomatic treatment (Bates et al., 2015). Pridopidine (ACR16) is emerging in clinical trials as a potential therapeutic to mitigate motor symptoms (*e.g.*, total motor score improvement was observed when tested as a secondary endpoint in two independent clinical trials) in HD patients (de Yebenes et al., 2011; Esmaeilzadeh et al., 2011; Huntington Study Group, 2013; Lundin et al., 2010). Pridopidine was initially identified as a stabilizer of the dopamine system, normalizing hyper- and hypodopaminergic behaviors, with the proposed mode of action of a D_2 receptor (D2R) antagonist, a partial weak agonist, or both a positive allosteric modulator and an orthosteric antagonist (Dyhring et al., 2010; Nilsson et al., 2004; Rung et al., 2008). However, the affinity of pridopidine for D2R is low (IC50 and Ki ~10 μM) (Dyhring et al., 2010) compared to its affinity for the sigma-1 receptor (S1R; Ki ~80 nM) (Sahlholm et al., 2013). Indeed, pridopidine exhibits efficient S1R binding, but not D2R binding, at behaviorally relevant doses *in vivo* (Sahlholm et al., 2015), indicating that the therapeutic mechanism of action for pridopidine may primarily involve the S1R.

S1R is a brain-enriched, transmembrane protein of 223 amino acids in the endoplasmic reticulum (ER) (Kourrich et al., 2012). S1R is evolutionarily conserved and lacks sequence homology with other mammalian proteins. Computational modeling and NMR studies indicate that S1R contains 2 transmembrane domains in ER membrane (Brune et al., 2014; Ortega-Roldan et al., 2015), although a recent crystal structure indicated a single transmembrane domain topology (Schmidt et al., 2016). S1R is often referred to as a “chaperone” (Su et al., 2010), but its primary function appears to involve modulation of ion channels (Kourrich et al., 2012). S1R is normally restricted to mitochondrial-associated membrane (MAM) domains where it regulates calcium (Ca^{2+}) signaling between the ER and mitochondria, as well as lipid transport (Hayashi and Su, 2003; Hayashi and Su, 2007). However, high concentrations of S1R agonists, or alternatively ER stress, lead to dislocation of S1R beyond the MAM domain (Su et al., 2010) so as to regulate ion channels on the

plasma membrane (Kourrich et al., 2012). Other roles have been reported for S1R in brain function, including neuromodulation (Maurice et al., 2006) and neuroplasticity (Kourrich et al., 2012; Takebayashi et al., 2004; Tang et al., 2009; Tsai et al., 2009).

S1R was first identified as a target for treating neuropsychiatric disorders, including drug addiction, depression and schizophrenia (Maurice and Su, 2009). Additional indications are now emerging from genetic data pertaining to neurodegenerative diseases, such as Alzheimer's disease (Fehér et al., 2012; Mishina et al., 2008; Uchida et al., 2005), amyotrophic lateral sclerosis (Al-Saif et al., 2011), hereditary motor neuropathy (Li et al., 2015) and frontotemporal lobar degeneration (Luty et al., 2010). Several studies have identified neuroprotective properties of S1R modulators (Fisher et al., 2016; Marrazzo et al., 2005; Ruscher et al., 2011; Schetz et al., 2007; Smith et al., 2008). In previous studies, the S1R agonist PRE-084 displayed neuroprotective properties in PC6.3 cells expressing N-terminal mHtt (Hyrskyluoto et al., 2013). Similarly, pridopidine improved motor performance and prolonged survival of R6/2 HD mice and exerted neuroprotective effects in a mouse striatal knock-in cellular model of HD ($STHdh^{111/111}$) (Squitieri et al., 2015). These data suggest that pridopidine might act as a disease-modifying therapeutic in HD by stimulating S1R activity.

Early neuropathological features of HD include perturbed corticostriatal synaptic function and connectivity (Miller and Bezprozvanny, 2010; Milnerwood and Raymond, 2007; Milnerwood and Raymond, 2010; Murmu et al., 2013; Orth et al., 2010; Schippling et al., 2009), eventually leading to overt neurodegeneration of medium spiny neurons (MSNs) in the striatum (Myers et al., 1988; Vonsattel and DiFiglia, 1998). Perturbed stability of synaptic spines has been suggested to underlie the development of HD symptoms (Bezprozvanny and Hiesinger, 2013; Murmu et al., 2013; Ryskamp et al., 2016). In recent studies, we demonstrated that post-synaptic dendritic spines of MSNs are lost in aged corticostriatal co-cultures established from YAC128 mice (Wu et al., 2016). In the present study, we used this *in vitro* HD MSN spine loss model to investigate the potential mechanism of action of pridopidine in HD and to assess S1R as a therapeutic target of pridopidine.

2. Materials and methods

2.1. Mice

Experiments involving mice were approved by the Institutional Animal Care and Use Committee of the University of Texas Southwestern Medical Center at Dallas and followed the National Institutes of Health Guidelines for the Care and Use of Experimental Animals. Wild type (WT; FVB/NJ) and YAC128 transgenic (FVB-Tg(YAC128)53Hay/J; Jackson Labs: stock # 004938) mice (Slow et al., 2003) were maintained at UT Southwestern Medical Center in barrier facility (12 h light/dark cycle) and genotyped as in (Wu et al., 2011).

2.2. Statistical analysis of the Q175 HD mouse model gene expression (CHDI allelic series six month dataset)

CAG knockin mouse RNAseq data were downloaded from the Cure Huntington's Disease Initiative (CHDI) website http://chdifoundation.org/datasets/ and were normalized using the voom transform from R package limma v3.18.13 in R v3.1.3. Using lmFit, genes were tested for differential expression in striata comparing between 6 months old Q20 (normal phenotype) and 6 months old Q175 heterozygotes. Q175 mice express an allele encoding the human HTT exon 1 sequence with a ~190 CAG repeat tract that replaces mouse Htt exon 1 and results in an HD phenotype.

2.3. Chronic treatment animal studies of gene expression profiles

Gene expression analysis of pridopidine-treated rats was recently described (Geva et al., 2016). Briefly, Sprague Dawley rats ($n = 6$) were treated daily by oral gavage with pridopidine (60 mg/kg) over 10 days. Six control Sprague Dawley rats were vehicle-treated. On the 10th day, 90 min following the last drug administration, brains were removed and RNA was isolated from the striatum of each rat and was analyzed using Affymetrix Rat 230_2 arrays. The gene expression data from 12 striatum samples was RMA normalized with affy package v1.42.3 in R v3.1.2. Probesets were annotated according to the Affymetrix Rat230_2 Release 22 annotation file. Processing of the Affymetrix data is detailed in the previous publication (Geva et al., 2016). The limma package v3.18.13 in R v3.1.3 was used to test if relevant calcium-related genes were differentially expressed between the two groups of biological replicates and multiple hypothesis testing was corrected for using the Bonferroni correction. Limma employs an empirical Bayes method to moderate standard error (Ritchie et al., 2015). When a gene had multiple probesets, the probeset with the highest absolute value of fold change was reported.

2.4. Western blot analysis

Striata from WT and YAC128 mice at 2, 6, and 12 months of age were isolated by dissection in PBS following euthanasia by euthasol injection and cervical dislocation. Cortices were similarly isolated for WT and YAC128 mice at 12 months of age. Human samples from caudate/nucleus accumbens/putamen and globus pallidus were obtained from the Harvard Brain Tissue Resource Center (http://www.brainbank.mclean.org/) and were processed as in (Sun et al., 2014). Isolated tissue was weighed and for each 100 mg of tissue, 200 µl of cold lysis buffer (1% CHAPS, 137 mM NaCl, 2.7 mM KCl, 4.3 mM Na_2HPO_4, 1.4 mM KH_2PO_4, pH 7.2, 5 mM EDTA, 5 mM EGTA, 1 mM PMSF, 50 mM NaF, 1 mM Na_3VO_4 and protease inhibitors) was used for homogenizing tissue and solubilizing protein (4 °C for 1 h). Samples were centrifuged at 10,000*g* for 10 min at 4 °C and the supernatant was transferred to a new tube. For human samples, the protein concentration was measured with a NanoDrop. Based on the volume of supernatant, an appropriate amount of 6 × SDS buffer was added to each sample. Human samples were diluted with 1 × SDS buffer based on the measured concentration of protein to standardize protein loading into the gel. For Western blot analysis of primary neuron cultures, WT and YAC128 striatal, cortical and corticostriatal cultures were aged to DIV21. Culture media was replaced with 1 × SDS lysis buffer. A pipette tip was used to scrape the bottoms of wells. Lysates were transferred to 1.5

ml tubes on ice and then sonicated. Samples were temporarily transferred from ice to a 90 °C tube rack for 3 min. The protein lysates were separated by SDS-PAGE and analyzed by Western blotting with mouse anti-S1R pAb (1:200, Santa Cruz, sc-137,075), mouse anti-calbindin-D-28K (1:500, clone CB-955, Sigma), rabbit anti-homer1a (1:500, Synaptic Systems, Cat. No. 160 013), and mouse anti-tubulin (1:5000, DSHB, E7-c). The homer1a antibody was validated by immunoblotting brain lysates from homer1a KO mice (*i.e.*, the ~28 kDa band was absent for homer1a KO brain samples). The HRP-conjugated anti-mouse secondary antibody (111–035-144) and anti-rabbit secondary antibody (115-035-146) were from Jackson ImmunoResearch. Data were densitometrically analyzed using ImageJ by normalizing the density of each band to tubulin signal of the same sample after subtracting the background.

2.5. In vitro spine loss assay

To study MSN spine loss *in vitro*, corticostriatal co-cultures were prepared from WT and heterozygous YAC128 littermates as in (Wu et al., 2016). Striata and cortices were dissected from pups on postnatal day 0–1 (in 1 × Hank's Balanced Salt Solution, 16.36 mM HEPES, 10 mM $NaHCO_3$, 1 × penicillin-streptomycin). Brain tissue was cut into small pieces (~500 μm chunks), centrifuged (800 rpm for 4 min), digested with papain dissolved in Neurobasal-A medium (30 min at 37 °C in 500 μl of 114 U papain/10 ml NBA; Worthington), rinsed and centrifuged (2000 rpm for 4 min; Neurobasal-A medium with 10% FBS and 25 μg/ml DNAse I), mechanically dissociated (in 500 μl of dissection media with 5 mg/ml DNAse I), rinsed and centrifuged (2000 rpm for 4 min; in dissection media then again in plating media), plated on poly-D-lysine coated 12 mm coverslips (0.5 ml/well of 0.1 mg/ml poly-D-lysine in PBS for 30 min at 37 °C, rinsed with dissection media then plating media and dried with the coverslips centered in each well) in 80 μl of Neurobasal-A medium supplemented with 5% FBS, 2% B27 and 0.5 mM L-glutamine (Invitrogen) for 7 min. Then an additional 920 μl of plating media was added to each well and cells were maintained at 37 °C in a 5% CO_2 incubator, feeding weekly by addition of 400 μl of NBA, 2% B27 and 0.5 mM L-glutamine. The anterior half of bilateral cortices from one brain and striata from three brains were used to plate 24 wells of a 24-well plate. The average plating densities were ~350 cells/mm^2 for cortical neurons (Ctx) and ~1060 cells/mm^2 for MSNs (a 3:1 MSN:Ctx ratio).

Drugs were dissolved in Neurobasal A media (NBA) from 10 mM stock solutions (DMSO) immediately prior to experiments. Starting on DIV21 co-cultures were treated with pridopidine or 3-PPP (100 nM or 1 μM). The compounds or the vehicle control (NBA + DMSO) were added directly to culture media from 10 μM NBA stocks. Cultures were fixed after 16 h of drug treatment and processed for immunohistochemistry. Co-cultures were fixed for 20 min in 4% formaldehyde plus 4% sucrose in PBS (pH 7.4; 4 °C), rinsed twice with cold PBS, permeabilized for 5 min in 0.25% Triton-X-100 (RT) and rinsed again with PBS (RT). Cultures were blocked with 5% BSA in PBS and immunostained with a rabbit anti-DARPP-32 antibody (1:500, Cell Signaling, 2306 s) and, after rinsing 3 × with PBS, a goat anti-rabbit Alexa488 secondary antibody (1:1000). DARPP32 is highly expressed in MSNs and can be immunolabeled to reliability visualize MSN spine morphology *in vitro* (Wu et al., 2016). Z-stacks were captured using a 63 × glycerol objective (N.A. 1.3) on a confocal microscope (Leica SP5) with the pinhole set to one airy unit. The density of

dendritic spines of DARPP32-positive MSNs was automatically quantified by using the NeuronStudio software package (Rodriguez et al., 2008) with manual correction. Spine shapes were categorized as described in (Wu et al., 2016). Data were analyzed from at least three batches of cultures for each experiment.

2.6. Lenti-virus preparation

We used a lenti-expression vector (FUGW; addgene.org/14883/) to drive expression of GFP or Cherry, lenti-Cas9-Blast (addgene.org/52962/) or lenti-GuidePuro (addgene.org/52963/). To generate lenti-viruses, plasmids of interest were mixed with lenti-viral production plasmids (Δ8.9 and VSVG) in 1 ml DMEM and 60 μl polyethylenimine (PEI) for 20 min at RT. Culture media (DMEM + 10% FBS) was replaced with 11.5 ml of NBA and the plasmid mixture was dripped into the fresh NBA media to transfect the HEK293T cells for virus production and packaging. This media was collected 48 h later, centrifuged (2000 RPM for 5 min), filtered (0.45 μm pore size) and aliquoted into cryotubes, which were flash-frozen in liquid nitrogen and stored at −80 °C until use. 100 μl of lenti-virus media was added to each well of neuron cultures on DIV7. Lenti-viruses produced through this approach exhibited selective neuronal tropism as revealed by GFP expression and MAP2 immunostaining, with a ~90% neuronal transfection rate (Wu et al., 2016).

2.7. CRISPR/Cas9-mediated deletion of S1R

To delete neuronal S1R in corticostriatal co-cultures we used the CRISPR/Cas9 system. GuideRNA sequences targeting mouse S1R were designed using bioinformatics tools (crispr.mit.edu for maximizing specificity and http://www.broadinstitute.org/rnai/public/analysis-tools/sgrna-design for selecting guide sequences with predicted efficacy) and sgRNA plasmids targeting S1R (gS1R) were generated. A sgRNA sequence targeting exon 1 of S1R (GCAGCTTGCTCGACAGTATG) was subcloned into the lentiGuide-Puro plasmid (addgene.org/52963/) as in (Sanjana et al., 2014) following their protocol (addgene.org/static/data/plasmids/52/52963/52963-attachment_IPB7ZL_hJcbm.pdf). The lenti-Cas9-Blast plasmid (addgene.org/52962/) was used to express Cas9. To validate these plasmids, MEF cells were co-transfected with Cas9-Blast and gS1R-Puro plasmids using FuGENE6 (1:4 DNA to charge ratio) and cells transfected with both plasmids were selected with 5 μg/ml blasticidin and 10 μg/ml puromycin in the culture media. Western blotting analysis confirmed efficient deletion of S1R in MEF cells. Western blotting and functional analysis in the spine loss and calcium imaging assays confirmed efficient deletion by Cas9 and gS1R in co-cultures. As in (Platt et al., 2014), a guideRNA sequence (GTGCGAATACGCCCACGCGAT) targeting the bacterial gene β-galactosidase (LacZ) was used as a negative control (gLacZ).

2.8. Fura-2 calcium imaging experiments

Fura-2 Ca^{2+} imaging experiments with corticostriatal co-cultures were performed as described previously (Wu et al., 2016) on DIV14–20. To distinguish cortical neurons from MSNs, in preparation of the co-culture, cortical neurons were plated on DIV0 and infected with lenti-GFP. 24 h later, media was replaced and striatal neurons were plated. GFP-negative striatal neurons were identified for analysis as in (Wu et al., 2016). The neurons were loaded with Fura-2-AM (5 μM; Molecular Probes) for 45 min at 37 °C and transferred

to a recording chamber filled with artificial cerebrospinal fluid (ACSF) (140 mM NaCl, 5 mM KCl, 1 mM $MgCl_2$, 2 mM $CaCl_2$, 10 mM HEPES [pH 7.3]). When Fura-2 fluorescence was evoked with 340 and 380 nm excitation produced from a DeltaRAM-X illuminator, 510 nm emissions were captured with an Evolve camera and EasyRatioPro software (Photon Technology International, Inc.) to measure the cytosolic calcium concentration (340F/380F ratio). To measure $InsP_3R1$-dependent Ca^{2+} release as described (Wu et al., 2016), external Ca^{2+} was removed and the basal calcium level (R_0 = 340F/380F at baseline) was recorded for 60 s prior to addition of 10 μM (*S*)-3,5-DHPG (Tocris). R = 340F/380F at peak response within 1 min of stimulus application. To measure the size of the ionomycin-sensitive Ca^{2+} pool, the neurons were washed with Ca^{2+}-free ACSF (100 μM EGTA) for 30 s prior to the application of 5 μM IO and the Ca^{2+} signals were recorded as R = 340F/380F. The ER Ca^{2+} pool size was calculated by integrating the area under the response curve as described (Wu et al., 2016).

2.9. GCaMP5G Ca^{2+} imaging experiments

GCaMP5-based Ca^{2+} imaging of MSN spines was performed as described (Wu et al., 2016). To distinguish cortical neurons from MSNs, corticostriatal co-cultures were prepared as in Fura-2 Ca^{2+} imaging experiments except that lenti-Cherry was used to infect cortical neurons. Co-cultures were transfected on DIV7 with a GCaMP5G expression plasmid (Jiang and Chen, 2006) using a CalPhos Transfection Kit (Clontech). MSNs in the co-cultures were identified as in (Wu et al., 2016) by GCaMP5 expression, morphology and lack of Cherry expression. GCaMP5 was imaged with an Olympus IX70 inverted epifluorescence microscope equipped with a 60 × lens, Cascade 650 digital camera (Roper Scientific) and Prior Lumen 200 illuminator (488 nm excitation). Images were collected at 0.5 Hz with MetaFluor (Universal Imaging). To measure neuronal store-operated Ca^{2+} entry (nSOC), the co-cultures were incubated in Ca^{2+}-free media containing 1 μM thapsigargin (Tg) and 400 μM EGTA for 5 min before returning to the ACSF containing 2 mM Ca^{2+}, 1 μM Tg and a Ca^{2+} channel inhibitor cocktail (1 μM TTX, 50 μM AP5, 10 μM CNQX and 50 μM nifedipine). The basal calcium level (F_0) in Ca^{2+}-free media was recorded for 40 s prior to Ca^{2+} add back. F = peak response from Ca^{2+} re-addition. Data analysis was performed using ImageJ (NIH).

2.10. Statistical analyses

Data are presented as mean ± SE and were statistically analyzed with GraphPad Prism 6 using two-way ANOVAs followed by a multiple comparisons test. Sidak's *post hoc* test was used when only comparing WT *vs*. YAC128 for each condition. Tukey's *post hoc* test was used to make all comparisons. Dunnett's *post hoc* test was used when comparing against the control condition. The multiplicity adjusted p value is reported. $p > 0.05$ = n.s, $p < 0.05$ = *, $p < 0.01$ = **, $p < 0.001$ = *** and $p < 0.0001$ = ****.

3. Results

3.1. Upregulation of striatal S1R in both mice and patients with advanced but not early HD

In order to evaluate striatal S1R expression in association with ER calcium dysregulation, we evaluated its protein levels in YAC128 HD mice by Western blotting. At 2 months,

normalized S1R expression in YAC128 striata (1.13 ± 0.2; $n = 10$ mice) was similar to WT striata (Fig. 1A, B; $n = 11$). As normalized to WT ($n = 12$), at 6 months S1R expression was slightly (not significantly) elevated in YAC128 striata (1.26 ± 0.19; $n = 10$) (Fig. 1A, B). By 12 months S1R expression was significantly upregulated in YAC128 striata (1.42 ± 0.1; $n = 12$) compared to WT striata ($p < 0.05$; $n = 12$; Sidak test) (Fig. 1A, B). By contrast, cortical S1R expression was similar in WT and YAC128 mice at 12 months of age (WT = 1 ± 0.18, $n = 6$; YAC128 = 0.93 ± 0.072, $n = 6$; $p > 0.05$; unpaired *t*-test). We also examined lysates from primary striatal cultures, cortical cultures and corticostriatal co-cultures from WT and YAC128 mice on DIV21. We observed no significant changes in S1R expression in WT *vs.* YAC128 cultures (WT striatal culture = 1 ± 0.15, $n = 3$; YAC128 striatal culture = 0.71 ±0.16, $n = 3$; WT cortical culture = 1 ± 0.12, $n = 3$; YAC128 cortical culture = 0.84 ± 0.2, $n = 3$; WT corticostriatal co-culture = 1 ± 0.16, $n = 4$; YAC128 corticostriatal co-culture = 0.985 ± 0.103 $n = 4$; $p > 0.05$; unpaired *t*-tests), indicating that HD-related changes in striatal S1R expression exclusively occur *in vivo*. We also evaluated S1R expression levels in samples from the basal ganglia of HD patients (HD3 = moderate HD; HD4 = advanced HD) compared to healthy controls (HC). S1R expression was moderately (not significantly) elevated in striatal samples from HD3 patients (1.46 ± 0.2; $n = 7$) compared to HC (1 ± 0.11; $n = 5$) (Fig. 1C, D). S1R expression was significantly upregulated in striatal samples from HD4 patients (2.21 ± 0.6; $n = 3$; $p < 0.05$; Sidak test) compared to HC (Fig. 1C, D). We also examined S1R expression in the human globus pallidus, which receives inputs from the caudate nucleus and putamen. S1Rwas slightly, but non-significantly upregulated in globus pallidus samples from HD3 and HD4 patients compared to healthy controls (HC = 1 ± 0.096, $n = 6$; HD3 = 1.4 ± 0.19, $n = 7$; HD4 = 1.65 ± 0.34, $n = 8$; $p > 0.05$; Dunnett's test). These data are consistent with a compensatory increase in striatal S1R expression in late HD not seen in early HD.

3.2. Pridopidine stabilizes MSN spines in aging YAC128 corticostriatal co-cultures via S1R

In previous studies, we developed an *in vitro* model of synaptic pathology in HD that is based on analysis of MSN spine density in corticostriatal co-cultures established from YAC128 mice. We demonstrated that YAC128 MSNs in these cultures display age-dependent spine loss when compared to WT MSNs (Wu et al., 2016). 3-PPP is a selective S1R agonist with a very similar chemical structure to pridopidine (Fig. 2A) and an identical affinity for S1R (Sahlholm et al., 2013). To evaluate whether S1R agonists can stabilize synaptic connections in HD, we administered 3-PPP to corticostriatal co-cultures from WT and YAC128 mice. Exposure to 100 nM and 1 μM 3-PPP had no effect on the density of WT MSN spines (WT = 10.5 ± 0.35 spines/10 μm of dendritic length, $n = 23$; WT 100 nM 3-PPP = 10.7 ± 0.54 spines/10 μm, $n = 8$; WT 1 μM 3-PPP = 10.8 ± 0.86 spines/10 μm, $n = 8$) (Fig. 2B, C). Compared to WT, the spine density in co-cultured MSNs from YAC128 mice was substantially reduced (YAC128 = 5.99 ± 0.26 spines/10 μm, $n = 23$; $p < 0.0001$) (Fig. 2B, C), which is consistent with our previous observations (Wu et al., 2016). 100 nM and 1 μM 3-PPP elevated the density of YAC128 MSN spines to WT levels (YAC128 100 nM 3-PPP = 11.0 ± 0.78 spines/10 μm, $n = 8$; YAC128 1 μM 3-PPP = 11.4 ± 0.61 spines/10 μm, $n = 8$) (Fig. 2B, C). Likewise, treatment with pridopidine had no effect on WT MSN spines (WT 100 nM pridopidine = 11.1 ± 0.52 spines/10 μm, $n = 15$; WT 1 μM pridopidine = 10.5 ± 0.47 spines/10 μm, $n = 15$), but rescued MSN spines in YAC128 co-cultures (YAC128 100

nM pridopidine = 9.6 ± 0.54 spines/10 μm, $n = 15$; YAC128 1 μM pridopidine = 10.3 ± 0.36 spines/10 μm, $n = 15$) (Fig. 2B, C). In this model, all spine types (mushroom, thin, stubby) are lost uniformly (Wu et al., 2016). Treatment with pridopidine uniformly rescued all spine types (data not shown). We also tested other S1R agonists, specifically PRE-084 and (−)-OSU6162, both of which also effectively rescued YAC128 MSN spines at 100 nM and 1 μM concentrations (data not shown).

To evaluate whether S1R is required for the synapto-protective effects of 3-PPP and pridopidine, we used the CRISPR/Cas9 system to delete S1R. Co-expression of Cas9 and guideRNA targeting the mouse S1R gene (gS1R) effectively deleted S1R in MEF cells, whereas co-expression of Cas9 and guideRNA targeting the bacterial β-galactosidase gene (gLacZ) preserved S1R expression (Fig. 3A).

To determine the molecular mechanism of pridopidine's synapto-protective effect, MSN spine analysis with corticostriatal co-cultures from YAC128 mice was performed following deletion of S1R by coinfecting cultured neurons on DIV7 with lenti-Cas9 and lenti-gS1R or lenti-gLacZ as a control (Fig. 3B, C). In our previous studies we used a similar approach to delete STIM2 in corticostriatal co-cultures (Wu et al., 2016).

In gLacZ cultures, the WT MSN spine density was 13.2 ± 0.68 spines/10 μm ($n = 7$) (Fig. 3B, C) and the YAC128 MSN spine density was reduced to 6.2 ± 0.73 spines/10 μm ($n = 7$) (Fig. 3B, C). Consistent with the previous results (Fig. 2B, C), 16-h treatment of DIV21 co-cultures with 100 nM 3-PPP or pridopidine had no effect on the density of MSN spines in WT gLacZ co-cultures (WT control = 13.2 ± 0.7 spines/10 μm, WT 3-PPP = 12.5 ± 1.8 spines/10 μm, WT pridopidine = 13.3 ± 0.8 spines/10 μm, $n = 3–7$, $p > 0.05$) and rescued MSN spine loss in YAC128 gLacZ co-cultures (YAC128 control = 6.2 ± 0.7 spines/10 μm, YAC128 3-PPP = 13.7 ± 1.1 spines/10 μm, YAC128 pridopidine = 12.7 ± 0.9 spines/10 μm, $n = 3–7$, $p < 0.0001$) (Fig. 3B, C). The spine density of MSNs in WT gS1R co-cultures was diminished to 5.83 ± 0.47 spines/10 μm ($n = 7$, $p < 0.0001$ compared to WT gLacZ), indicating that S1R has a physiological role in maintaining MSN spine stability.

Although 3-PPP and pridopidine rescue YAC128 MSN spines (Figs. 2B, C and 3B, C), 3-PPP and pridopidine were unable to prevent WT MSN spine loss in the absence of S1R (WT gS1R + 3-PPP = 7.42 ± 0.89 spines/10 μm, $n = 3$, $p < 0.0001$ compared to WT gLacZ; WT gS1R + pridopidine = 6.34 ± 0.35 spines/10 μm, $n = 4$, $p < 0.0001$ compared to WT gLacZ). This is consistent with a crucial role for S1R in mediating the synapto-protective effects of 3-PPP and pridopidine.

Although co-expression of Cas9 and gS1R in WT co-cultures caused MSN spine loss, their co-expression in YAC128 co-cultures did not cause additional spine loss beyond that caused by mHtt (YAC128 gS1R = 7.42 ± 0.61 spines/10 μm, $n = 7$, $p > 0.05$ compared to YAC128 gLacZ). Even though 3-PPP and pridopidine restored the density of MSN spines to WT levels in YAC128 gLacZ co-cultures ($n = 3–7$, $p < 0.0001$ compared to YAC128 gLacZ), they were unable to rescue MSN spines in YAC128 gS1R co-cultures (YAC128 gS1R + 3-PPP = 7.41 ± 1.19 spines/10 μm, $n = 3$, $p > 0.05$; YAC128 gS1R + pridopidine = 5.57 ± 0.90 spines/10 μm, $n = 4$, $p > 0.05$) (Fig. 3B, C).

This indicates that S1R is required for the protective effects of both 3-PPP and pridopidine. These results are consistent with the hypothesis that pridopidine rescues spines in HD neurons by activating S1R.

3.3. Pridopidine normalizes ER Ca^{2+} homeostasis in MSNs from YAC128 corticostriatal co-cultures

Our recent data demonstrated that synaptic store-operated calcium entry (nSOC) plays an important role in control of stability of hippocampal (Popugaeva et al., 2015; Sun et al., 2014; Zhang et al., 2015) and striatal (Wu et al., 2016) synaptic spines. In HD, mHtt binds to and sensitizes $InsP_3R1$ to basal levels of $InsP_3$ (Tang et al., 2003), increasing Ca^{2+} leakage from the ER (Tang et al., 2005; Tang et al., 2003). This leads to excessively elevated SOC in MSNs (Wu et al., 2011), an effect that is more pronounced in MSN spines (Wu et al., 2016). This tonic Ca^{2+} signal is synaptotoxic, contributing to MSN spine loss in the YAC128 HD mouse model *in vitro* and *in vivo* (Wu et al., 2016). S1R is known to modulate intracellular Ca^{2+} signaling (Hayashi and Su, 2007; Srivats et al., 2016). In the next series of experiments we evaluated effects of pridopidine on MSN Ca^{2+} homeostasis.

We previously demonstrated that DHPG-evoked Ca^{2+} release from the ER in MSNs is mediated by $InsP_3R1$ and that DHPG-evoked Ca^{2+} release is enhanced in YAC128 MSNs in corticostriatal co-cultures (Wu et al., 2016). After removing external Ca^{2+}, the application of 10 μM DHPG to corticostriatal co-cultures evoked a cytosolic Ca^{2+} elevation in the somata of Fura-2-loaded MSNs (Fig. 4A, B). The amplitude of Ca^{2+} release in these experiments was very low in WT MSNs but was elevated significantly in YAC128 MSNs (Fig. 4A). On average, the amplitude of DHPG-induced response was 1 ± 0.139 (n = 153 MSNs) in WT MSNs and 8.52 ± 0.804 (n = 185) in YAC128 MSNs ($p < 0.0001$), consistent with our previous report (Wu et al., 2016). 16–24 h pre-incubation of co-cultures with 1 μM Pridopidine had no effect on Ca^{2+} release in WT MSNs (0.551 ± 0.079, n = 175, $p > 0.05$), but suppressed Ca^{2+} release in YAC128 MSNs to WT levels (1.27 ± 0.101, n = 398, $p > 0.05$) (Fig. 4A, B). These results indicated that incubation with pridopidine suppresses supranormal activity of the $InsP_3R1$ in mHtt-expressing MSNs.

Because pridopidine normalizes $InsP_3R1$ hyperactivity, it would be expected to reduce the leakage of Ca^{2+} from the ER in YAC128 MSNs and therefore increase ER Ca^{2+} content. To measure ER Ca^{2+} content in the somata of Fura-2-loaded MSNs in corticostriatal co-cultures, extracellular Ca^{2+} was removed and then ionomycin (IO) was added to release Ca^{2+} from the internal stores. ER Ca^{2+} content was quantified by measuring the area under the IO-evoked Ca^{2+} response curve. As we previously reported (Wu et al., 2016), the ER Ca^{2+} levels were substantially depleted in YAC128 control MSNs (YAC128 gLacZ 0.49 ± 0.038, n = 116, $p > 0.05$) compared to WT control MSNs (WT gLacZ 1 ± 0.036, n = 173, $p < 0.01$) (Fig. 5A–C). Pre-incubation of co-cultures with 1 μM pridopidine for 16–24 h non-significantly increased ER Ca^{2+} content in WT co-cultures (WT gLacZ + pridopidine 1.19 ± 0.036, n = 225), but significantly repleted ER Ca^{2+} in YAC128 MSNs (YAC128 gLacZ + pridopidine 1.12 ± 0.078, n = 94, $p < 0.0001$) (Fig. 5A–C).

To evaluate the potential role of S1R in mediating effects of pridopidine on MSN Ca^{2+} homeostasis, we used the CRISPR/Cas9 system to delete neuronal S1R and measured the

effect of pridopidine on ER Ca^{2+} levels. Co-infection of WT corticostriatal co-cultures with lenti-Cas9 and lenti-gS1R suppressed ER Ca^{2+} levels (WT gS1R 0.59 ± 0.04, $n = 103$, $p < 0.001$) (Fig. 5A–C), indicating that basal S1R activity may partially attenuate tonic Ca^{2+} leakage in MSNs. Even though pridopidine treatment slightly elevated ER Ca^{2+} levels in WT gLacZ MSNs, this effect was absent when S1R was deleted (WT gS1R + pridopidine, 0.60 ± 0.063, $n = 76$, $p > 0.05$) (Fig. 5A–C). Deletion of S1R had no additional effect on ER Ca^{2+} levels in YAC128 MSNs (YAC128 gS1R, 0.50 ± 0.03, $n = 92$, $p > 0.05$ compared to YAC128 gLacZ) (Fig. 5A–C), indicating that endogenous S1R is unable to adequately regulate ER Ca^{2+} levels in YAC128 MSNs without stabilization from S1R ligands. Additionally, the ability of pridopidine to elevate YAC128 ER calcium to WT levels was lost in the absence of S1R (YAC128 gS1R + pridopidine, 0.419 ± 0.038, $n = 95$, $p > 0.05$ compared to YAC128 gLacZ) (Fig. 5A–C). This indicates that the ability of pridopidine to restore ER Ca^{2+} homeostasis in YAC128 MSNs requires S1R.

3.4. Pridopidine normalizes spine nSOC in YAC128 MSNs from corticostriatal co-cultures

To compensate for constantly depleted ER calcium levels, YAC128 MSNs upregulate nSOC to replenish ER calcium stores (Wu et al., 2011). The nSOC pathway is particularly enhanced in synaptic spines of YAC128 MSNs, leading to spine loss (Wu et al., 2016). We therefore examined whether incubating co-cultures with 1 μM 3-PPP or pridopidine for 16 h, an amount of time sufficient to rescue spines, would suppress the hyperactive nSOC pathway in the spines of YAC128 MSNs.

As previously reported (Wu et al., 2016), MSN spine nSOC was enhanced in corticostriatal co-cultures from YAC128 mice (2.33 ± 0.15, $n = 110$ spines) when compared to that from WT mice (1 ± 0.089, $n = 110$, $p < 0.0001$) (Fig. 6A, B). 3-PPP, but not pridopidine, slightly reduced spine nSOC in WT MSNs (WT + 3-PPP = 0.47 ± 0.06, $n = 97$, $p < 0.01$; WT + pridopidine = 0.98 ± 0.14, $n = 70$, $p > 0.05$) (Fig. 6A, B). Both 3-PPP and pridopidine suppressed supranormal spine nSOC in YAC128 MSNs approximately to WT levels (YAC128 + 3-PPP = 0.59 ± 0.058, $n = 109$, $p < 0.05$; YAC128 + pridopidine = 0.77 ± 0.079, $n = 110$, $p > 0.05$) (Fig. 6A, B). From these results, we concluded that suppression of supranormal nSOC may contribute to synaptoprotective effects of 3-PPP and pridopidine in the YAC128 corticostriatal co-culture model of HD (Fig. 2).

3.5. Effects of pridopidine on striatal Ca^{2+} gene expression

To gain further insight into the role of pridopidine in regulation of calcium signaling, we used previously published data (Geva et al., 2016) to analyze changes in Ca^{2+} signaling gene expression profiles in rat striatum induced by chronic pridopidine therapy. In addition, we leveraged publically available striatum RNAseq data from the Q175KI mouse model for HD (Q175), and examined whether any calcium regulatory genes were downregulated in this model as compared to the control Q25KI mouse (Q25).

Notably, calbindin (Calb1) mRNA was upregulated in rat striatum following 10 days of oral pridopidine treatment ($p < 0.01$; adj. $p = 0.4$) (Fig. 7A), and it was downregulated in Q175 mice compared with Q25 ($p < 0.001$; adj. $p < 0.01$) (Fig. 7B). Calbindin functions as a buffer

for excessive intracellular calcium, and its downregulation is expected to predispose HD MSNs to Ca^{2+} overload (Kiyama et al., 1990).

To substantiate observations of mRNA, we examined calbindin protein expression in the striatum of untreated YAC128 mice by Western blotting. At 2 months of age, calbindin expression was similar in WT and YAC128 striata (WT = 1.0 ± 0.14, n = 3 mice; YAC128 = 0.87 ± 0.14, n = 3 mice; Fig. 7C–D). Likewise, calbindin expression was similar in WT and YAC128 striata at 6 months of age (WT = 1.0 ± 0.061, n = 12 mice; YAC128 = 0.79 ± 0.091, n = 11 mice; Fig. 7C–D). Similar to findings with Q175 mice, striatal calbindin was significantly downregulated in YAC128 mice at 12 months of age (WT = 1.0 ± 0.05, n = 12 mice; YAC128 = 0.67 ± 0.08, n = 11 mice; $p < 0.01$, Fig. 7C–D).

We also found that homer1a mRNA was upregulated in rat striatum post-pridopidine treatment ($p < 0.0001$; adj. $p < 0.05$, Fig. 7E), and it was downregulated in Q175 *vs.* Q25 (WT) mice ($p < 0.0001$; adj. $p < 0.001$, Fig. 7F). When analyzed by Western blotting, in striatal samples from untreated YAC128 mice, homer1a protein expression was similar at 2 months (WT = 1 ± 0.22, n = 4; YAC128 = 1.03 ± 0.16, n = 7) and 6 months (WT = 1 ± 0.18, n = 12; YAC128 = 0.93 ± 0.14, n = 11) of age, but was significantly downregulated at 12 months of age (WT = 1 ± 0.18, n = 13; YAC128 = 0.46 ± 0.09, n = 14; $p < 0.05$; Fig. 7C, G).

Homer proteins (Homer 1–3) are postsynaptic scaffolding proteins that are known to play a central role in calcium signaling by forming multi-protein complexes with calcium regulators including $InsP_3R1$, mGluR1/5 and Shank (Jardin et al., 2013; Shiraishi-Yamaguchi and Furuichi, 2007; Worley et al., 2007). Homer1a is a truncated splice-variant that acts as a dominant negative regulator of the full length homer proteins by preventing physical coupling and juxtaposition of mGluR1/5-Homer1-$InsP_3R1$ complex components, thereby attenuating Ca^{2+} release from the ER (Jardin et al., 2013; Shiraishi-Yamaguchi and Furuichi, 2007; Worley et al., 2007). Thus, the pridopidine-induced increase in Homer1a expression level may help to stabilize Ca^{2+} dysregulation in HD MSNs by reducing $InsP_3R1$-mediated Ca^{2+} release.

4. Discussion

We report here that S1R is upregulated in the striatum of both mice and patients with advanced but not early HD. This may reflect a compensatory response to mitigate the effects of ER Ca^{2+} dysregulation and synaptic instability. Consistent with this, treatment of corticostriatal co-cultures prepared from YAC128 mice with the S1R agonist 3-PPP prevented age-dependent MSN spine loss. Likewise, pridopidine improved synaptic connectivity in this *in vitro* model of HD, whereas S1R deletion decreased the density of WT MSN spines to YAC128 MSN levels without causing additional spine loss in YAC128 MSNs. The synapto-protective property of these compounds was eliminated by neuronal deletion of S1R, suggesting that 3-PPP and pridopidine bolster synaptic connections by stimulating S1R activity.

Given the role of S1R in the regulation of ER Ca^{2+} signaling (Hayashi and Su, 2007; Srivats et al., 2016), we evaluated whether 3-PPP and pridopidine stabilize calcium homeostasis in

co-cultured YAC128 MSNs. 16–24 hour treatment with pridopidine suppressed DHPG-induced Ca^{2+} release in YAC128 MSNs to WT levels. Pridopidine also elevated ER Ca^{2+} levels in YAC128 MSNs to WT levels, a S1R-dependent effect. Overnight treatment with 3-PPP or pridopidine reduced nSOC signaling in YAC128 MSN spines below synaptotoxic levels. These results suggest that pridopidine may prevent spine loss in YAC128 MSNs by modulating ER Ca^{2+} homeostasis. Moreover, the Ca^{2+} regulatory proteins calbindin and homer1a were upregulated in the striatum of rats following chronic pridopidine treatment, whereas their expression was downregulated in the striatum of aged Q175 and YAC128 mice. These transcriptional/translational changes may further fine tune Ca^{2+} signaling and synaptic stability.

4.1. S1R is necessary for formation and stability of MSN spines

Previous studies suggested that S1R plays an important role in the development and stability of dendritic spines in hippocampal neurons, as well as in the control of neuronal oxidative stress and Rac GTP signaling (Tsai et al., 2009). More recently, a microarray approach was used to evaluate transcriptional changes following RNAi knockdown of S1R in cultured hippocampal neurons (Tsai et al., 2012). S1R knockdown primarily affected pathways involved in sterol biosynthesis, protein ubiquitination, the actin cytoskeleton network, and oxidative stress (Tsai et al., 2012).

The potential role of S1R in the response to oxidative stress was corroborated by analysis of liver tissues and retinal glial cells from S1R knockout mice (Pal et al., 2012; Wang et al., 2015a) and may be important for dendritic spine stability in the hippocampus given that spine loss from S1R knockdown was rescued by reducing oxidative stress (Tsai et al., 2009). Consistent with important neuronal functions of S1R, S1R knockout mice are viable (Langa et al., 2003), but exhibit late-onset neurodegeneration (Bernard-Marissal et al., 2015; Ha et al., 2011; Mavlyutov et al., 2010). We demonstrate here that genetic ablation of S1R using the CRISPR/Cas9 system resulted in MSN spine loss in WT corticostriatal co-cultures, identifying an essential role of S1R in the development and/or maintenance of synaptic connections between cortical and striatal neurons.

4.2. Role of S1R in neurodegenerative disorders

Considering the important role of S1R in synaptic biology, it is not surprising that an important role of S1R is emerging in neurodegenerative diseases, such as Alzheimer's disease (Fehér et al., 2012; Maruszak et al., 2007; Mishina et al., 2008; Uchida et al., 2005), amyotrophic lateral sclerosis (Al-Saif et al., 2011; Belzil et al., 2013) and frontotemporal lobar degeneration (Luty et al., 2010). The mechanistic basis for these connections is starting to be elucidated (Nguyen et al., 2015). For example, it was recently demonstrated that S1R promotes turnover of p35, an activator of cyclin-dependent kinase 5 (cdk5) (Tsai et al., 2015). This function of S1R is connected with its ability to control phosphorylation of tau protein (Tsai et al., 2015) and may be responsible for the connection between reduced S1R function and Alzheimer's disease.

We observed herein upregulation of S1R in striatal samples from aged YAC128 HD mice and patients with severe HD. Striatal S1R upregulation may occur as a compensatory

response to chronic ER Ca^{2+} depletion (Hayashi and Su, 2007) in HD MSNs and, possibly, to synaptic dysfunction. Thus, changes in striatal S1R expression could represent a marker of HD progression. This was evident with the non-significant elevation of S1R protein in the basal ganglia of patients with HD3 (defined in (Shoulson and Fahn, 1979)), and would become significant with patients featuring more advanced pathology and atrophy (HD4). Given that S1R levels can be assessed in human patients using PET (Mishina et al., 2008), this may have implications for defining the optimal therapeutic window for pridopidine therapy and/or personalizing treatment. Interestingly, striatal S1R mRNA expression was unchanged in Q175 mice compared to Q20 controls at 6 months of age ($p = 0.653$; CHDI RNAseq dataset). Thus, the upregulation of striatal S1R in HD may result from changes in S1R translation and/or degradation. Either way, the trend toward a compensatory increase of S1R protein with progression of disease may also highlight the timing for treatment with pridopidine, with earlier treatment potentially of greater and more beneficial effect.

4.3. S1R as a target for pridopidine in HD

S1R agonists enhance cognitive performance, synaptic plasticity and neuronal survival in conditions of neuronal stress (Antonini et al., 2011; Antonini et al., 2009; Hindmarch and Hashimoto, 2010; Ruscher et al., 2011). Pharmacological activation of S1R was beneficial in experimental models of Parkinson's disease (Francardo et al., 2014) and Alzheimer's disease (Fisher et al., 2016; Marrazzo et al., 2005; Meunier et al., 2006; Villard et al., 2009). The S1R agonist PRE-084 exerted neuroprotective effects in PC6.3 cells expressing N-terminal mHtt (Hyrskyluoto et al., 2013). Pridopidine improved motor performance and prolonged survival of R6/2 HD mice and exerted neuroprotective effects in a mouse striatal knock-in cellular HD model ($STHdh^{111/111}$) (Squitieri et al., 2015). In our experiments, pridopidine and the chemically similar S1R agonist 3-PPP rescued MSN spine loss in YAC128 cortico-striatal co-cultures. Genetic ablation of S1R prevented the rescue of YAC128 MSN spines by 3-PPP and pridopidine, suggesting that S1R is a target for these compounds. This is consistent with the high affinity of 3-PPP and pridopidine for S1R (Sahlholm et al., 2013; Sahlholm et al., 2015). Our results suggest that the beneficial actions of pridopidine are likely to be mediated *via* activation of S1R, resulting in bolstering of HD MSN spines. These data suggest that pridopidine might act as a disease-modifying therapeutic in HD by stimulating S1R activity.

4.4. Effects on Ca^{2+} signaling from S1R activation by pridopidine

As discussed above, stimulation of S1R activity by pridopidine may lead to remodeling of the actin cytoskeleton in spines and/or a reduction in oxidative stress (Tsai et al., 2012). Another well-established function of S1R is to control ER Ca^{2+} signaling. It was demonstrated that S1R regulates $InsP_3R3$-mediated ER-mitochondrial Ca^{2+} transfer (Hayashi and Su, 2007) and removes the inhibitory actions of ankyrin on $InsP_3R3$ (Wu and Bowen, 2008). However, these actions of S1R appear to be specific for $InsP_3R3$ isoform, whereas $InsP_3R1$ is a predominant neuronal isoform (Taylor et al., 1999). S1R directly binds to $InsP_3R1$, but no direct functional effects on $InsP_3R1$ activity were observed in experiments with hepatocytes (Abou-Lovergne et al., 2011). It was concluded that activation of S1R leads to stimulation of PKC activity and suppression of $InsP_3$ synthesis in hepatocytes (Abou-Lovergne et al., 2011).

We previously discovered that mHtt enhances the sensitivity of $InsP_3R1$ to $InsP_3$, resulting in a tonic calcium leakage that decreases ER Ca^{2+} levels (Tang et al., 2009; Tsai et al., 2009; Tang et al., 2005; Tang et al., 2003). This overactivates STIM2-depedendent store-operated Ca^{2+} entry (SOC) in YAC128 MSN spines, causing spine loss (Wu et al., 2016). In our experiments herein, we discovered that incubation with pridopidine normalized ER Ca^{2+} release, ER Ca^{2+} levels and spine SOC in corticostriatal co-cultures from YAC128 mice. Moreover, incubation with pridopidine was sufficient to restore ER Ca^{2+} levels in YAC128 MSNs in a S1R-dependent manner.

Actions of pridopidine in these experiments could be mediated by stabilizing effects on $InsP_3R1$ function, by stimulation of PKC activity or by a different mechanism. Overnight treatment with pridopidine was sufficient to normalize ER Ca^{2+} levels and the enhanced nSOC pathway in YAC128 MSN spines. Of potential relevance to these findings, knockdown of S1R by RNAi was reported to affect expression levels of the SOC channel subunit Orai1 (Tsai et al., 2012). It has been reported that S1R overexpression or incubation with S1R agonists suppresses SOC in various cell lines (Brailoiu et al., 2016; Srivats et al., 2016). To explain these results it has been proposed that S1R may suppress SOC by binding to STIM1 and obstructing the interaction of STIM1 and Orai1 (Srivats et al., 2016). However, in our experiments pridopidine elevated ER Ca^{2+} levels in YAC128 MSNs, which would decouple STIMs from SOC channels. Thus, the attenuation of supranormal nSOC in YAC128 MSN spines by pridopidine is more likely to be explained by its effects on ER Ca^{2+} handling, although direct association of S1R with STIM1 and/or STIM2 may also contribute to the observed effects. Collectively, our findings suggest that the ability of pridopidine to stabilize corticostriatal synaptic connections involves normalization of synaptic Ca^{2+} signaling.

Analysis of genes that regulate Ca^{2+} revealed that calbindin and homer1a are upregulated in the striatum of rats following chronic pridopidine treatment and reciprocally downregulated in the striatum of Q175 mice. In Western blotting experiments we confirmed that these proteins are downregulated in the striatum of aged YAC128 mice. Calbindin, which chelates cytosolic Ca^{2+}, is absent in HD postmortem brain neurons (Kiyama et al., 1990), suggesting that loss of Ca^{2+} buffering is associated with disease progression and severity. Increased calbindin expression from pridopidine treatment should increase the cytosolic Ca^{2+} buffering capacity in HD MSNs and exert protective effects, as has been demonstrated in variety of neuronal insult models (Hugon et al., 1996; Yamada et al., 1990; Yenari et al., 2001).

Homer1a is a neuronal, activity-dependent, immediate early gene that suppresses mGluR1/5-induced ER Ca^{2+} release *via* $InsP_3Rs$ by preventing full length Homer1-mediated coupling between mGluR1/5 and $InsP_3Rs$ (Ango et al., 2001; Mao et al., 2005; Tu et al., 1998). Upregulation of Homer1a is expected to suppress excessive ER Ca^{2+} release in HD MSNs, leading to restoration of ER Ca^{2+} levels and reduced SOC. In support of this hypothesis, Homer1a overexpression suppressed mGluR activity and clustering in various cell culture assays (Ango et al., 2000; Ciruela et al., 1999; Roche et al., 1999; Tadokoro et al., 1999). Increased Homer1a expression attenuated neuronal injury induced by mGluR1 activation in a model of traumatic brain injury (Luo et al., 2014) and reduced Ca^{2+} overload and neuronal

injury in a MPP(+)-toxicity model with cultured rat mesencephalic cells (Zeng et al., 2013). Increased Homer1a expression was also recently demonstrated to exert neuroprotective effects against NMDA-induced neuronal injury (Wang et al., 2015b). Interestingly, expression of homer1a has been shown to be elevated following inhibition of neuronal SOC in PC12 cells, suggesting potential cross-talk between SOC and Homer1a expression in neuronal cells (Li et al., 2013). From these results we conclude that observed changes in expression of calbindin1 and homer1a may further contribute to the long-term beneficial effects of pridopidine in HD.

5. Conclusions

Pridopidine and 3-PPP are proposed to prevent Ca^{2+} dysregulation and synaptic loss in a YAC128 corticostriatal co-culture model of HD. The actions of pridopidine in striatal neurons are mediated by S1R and involve stabilization of ER Ca^{2+} levels, reduction of synaptic store-operated Ca^{2+} entry, and increased expression of the Ca^{2+} regulating proteins calbindin1 and homer1a. These results reveal a new potential mechanism of action for pridopidine and highlight S1R as a potential target for HD therapy.

Acknowledgments

TEVA Pharmaceuticals provided funding for the study. M.G., I.G. and M.H are employees of TEVA Pharmaceuticals and I.B. is a paid consultant to TEVA Pharmaceuticals.

We thank Leah Taylor for administrative assistance and Pippa Loupe for editorial assistance. We thank Drs. Paul Worley and Tao Xu (John Hopkins University) for providing samples of Homer 1a knockout brains. The research described herein was supported by TEVA Pharmaceuticals (SRA #109415) and by the National Institute of Neurological Disorders and Stroke of the National Institutes of Health (R01NS074376 and R01NS056224, IB; F32NS093786, DAR). IB holds the Carl J. and Hortense M. Thomsen Chair in Alzheimer's Disease Research.

Abbreviations

HD	Huntington disease
Htt	Huntingtin
MSN	medium spiny neuron
S1R	sigma-1 receptor
ER	endoplasmic reticulum
YAC128	yeast artificial chromosome 128Q expansion mice
3-PPP	R(+)-3-(3-Hydroxyphenyl)-*N*-propylpiperidine hydrochloride
SOC	store-operated calcium current
MAM	mitochondrial-associated membrane
gLacZ	guideRNA targeting the bacterial β-galactosidase gene
gS1R	guideRNA targeting the mouse S1R gene

MEF	mouse embryonic fibroblasts
DHPG	(*S*)-3,5-dihydroxyphenylglycine
IO	ionomycin

References

Abou-Lovergne A, Collado-Hilly M, Monnet FP, Koukoui O, Prigent S, Coquil JF, Dupont G, Combettes L. Investigation of the role of sigma1-receptors in inositol 1,4,5-trisphosphate dependent calcium signaling in hepatocytes. Cell Calcium. 2011; 50:62–72. [PubMed: 21641033]

Al-Saif A, Al-Mohanna F, Bohlega S. A mutation in sigma-1 receptor causes juvenile amyotrophic lateral sclerosis. Ann. Neurol. 2011; 70:913–919. [PubMed: 21842496]

Ango F, Pin JP, Tu JC, Xiao B, Worley PF, Bockaert J, Fagni L. Dendritic and axonal targeting of type 5 metabotropic glutamate receptor is regulated by homer1 proteins and neuronal excitation. J. Neurosci. 2000; 20:8710–8716. [PubMed: 11102477]

Ango F, Prézeau L, Muller T, Tu JC, Xiao B, Worley PF, Pin JP, Bockaert J, Fagni L. Agonist-independent activation of metabotropic glutamate receptors by the intracellular protein Homer. Nature. 2001; 411:962–965. [PubMed: 11418862]

Antonini V, Marrazzo A, Kleiner G, Coradazzi M, Ronsisvalle S, Prezzavento O, Ronsisvalle G, Leanza G. Anti-amnesic and neuroprotective actions of the sigma-1 receptor agonist (−)-MR22 in rats with selective cholinergic lesion and amyloid infusion. J. Alzheimers Dis. 2011; 24:569–586. [PubMed: 21297260]

Antonini V, Prezzavento O, Coradazzi M, Marrazzo A, Ronsisvalle S, Arena E, Leanza G. Anti-amnesic properties of (±)-PPCC, a novel sigma receptor ligand, on cognitive dysfunction induced by selective cholinergic lesion in rats. J. Neurochem. 2009; 109:744–754. [PubMed: 19245662]

Bates GP, Dorsey R, Gusella JF, Hayden MR, Kay C, Leavitt BR, Nance M, Ross CA, Scahill RI, Wetzel R, Wild EJ, Tabrizi SJ. Huntington disease. Nat. Rev. Dis. Primers. 2015; 1:15005. [PubMed: 27188817]

Belzil VV, Daoud H, Camu W, Strong MJ, Dion PA, Rouleau GA. Genetic analysis of SIGMAR1 as a cause of familial ALS with dementia. Eur. J. Hum. Genet. 2013; 21:237–239. [PubMed: 22739338]

Bernard-Marissal N, Médard JJ, Azzedine H, Chrast R. Dysfunction in endoplasmic reticulum-mitochondria crosstalk underlies SIGMAR1 loss of function mediated motor neuron degeneration. Brain. 2015; 138:875–890. [PubMed: 25678561]

Bezprozvanny I, Hiesinger PR. The synaptic maintenance problem: membrane recycling, Ca^{2+} homeostasis and late onset degeneration. Mol. Neurodegener. 2013; 8:23. [PubMed: 23829673]

Brailoiu GC, Deliu E, Console-Bram LM, Soboloff J, Abood ME, Unterwald EM, Brailoiu E. Cocaine inhibits store-operated Ca^{2+} entry in brain microvascular endothelial cells: critical role for sigma-1 receptors. Biochem. J. 2016; 473:1–5. [PubMed: 26467159]

Brune S, Schepmann D, Klempnauer KH, Marson D, Dal Col V, Laurini E, Fermeglia M, Wunsch B, Pricl S. The sigma enigma: in vitro/in silico site-directed mutagenesis studies unveil sigma1 receptor ligand binding. Biochemistry. 2014; 53:2993–3003. [PubMed: 24766040]

Ciruela F, Soloviev M, McIlhinney R. Co-expression of metabotropic glutamate receptor type 1α with Homer-1a/Vesl-1S increases the cell surface expression of the receptor. Biochem. J. 1999; 341:795–803. [PubMed: 10417346]

Dyhring T, Nielsen EØ, Sonesson C, Pettersson F, Karlsson J, Svensson P, Christophersen P, Waters N. The dopaminergic stabilizers pridopidine (ACR16) and (−)-OSU6162 display dopamine D(2) receptor antagonism and fast receptor dissociation properties. Eur. J. Pharmacol. 2010; 628:19–26. [PubMed: 19919834]

Esmaeilzadeh M, Kullingsjö J, Ullman H, Varrone A, Tedroff J. Regional cerebral glucose metabolism after pridopidine (ACR16) treatment in patients with Huntington disease. Clin. Neuropharmacol. 2011; 34:95–100. [PubMed: 21586914]

Fehér Á, Juhász A, László A, Kálmán J, Pákáski M, Janka Z. Association between a variant of the sigma-1 receptor gene and Alzheimer's disease. Neurosci. Lett. 2012; 517:136–139. [PubMed: 22561649]

Fisher A, Bezprozvanny I, Wu L, Ryskamp DA, Bar-Ner N, Natan N, Brandeis R, Elkon H, Nahum V, Gershonov E, LaFerla FM. AF710B, a novel M1/σ1 agonist with therapeutic efficacy in animal models of Alzheimer's disease. Neurodegener. Dis. 2016; 16:95–110. [PubMed: 26606130]

Foroud T, Gray J, Ivashina J, Conneally PM. Differences in duration of Huntington's disease based on age at onset. J. Neurol. Neurosurg. Psychiatry. 1999; 66:52–56. [PubMed: 9886451]

Francardo V, Bez F, Wieloch T, Nissbrandt H, Ruscher K, Cenci MA. Pharmacological stimulation of sigma-1 receptors has neurorestorative effects in experimental parkinsonism. Brain. 2014; 137:1998–2014. [PubMed: 24755275]

Geva M, Kusko R, Soares H, Fowler KD, Birnberg T, Barash S, Wagner AM, Fine T, Lysaght A, Weiner B, Cha Y, Kolitz S, Towfic F, Orbach A, Laufer R, Zeskind B, Grossman I, Hayden MR. Pridopidine activates neuroprotective pathways impaired in Huntington disease. Hum. Mol. Genet. 2016 (ddw238).

Ha Y, Saul A, Tawfik A, Williams C, Bollinger K, Smith R, Tachikawa M, Zorrilla E, Ganapathy V, Smith SB. Late-onset inner retinal dysfunction in mice lacking sigma receptor 1 (σR1). Invest. Ophthalmol. Vis. Sci. 2011; 52:7749–7760. [PubMed: 21862648]

Hayashi T, Su TP. σ-1 receptors (σ1 binding sites) form raft-like microdomains and target lipid droplets on the endoplasmic reticulum: roles in endoplasmic reticulum lipid compartmentalization and export. J. Pharmacol. Exp. Ther. 2003; 306:718–725. [PubMed: 12730355]

Hayashi T, Su TP. Sigma-1 receptor chaperones at the ER-mitochondrion interface regulate Ca(2+) signaling and cell survival. Cell. 2007; 131:596–610. [PubMed: 17981125]

Hindmarch I, Hashimoto K. Cognition and depression: the effects of fluvoxamine, a sigma-1 receptor agonist, reconsidered. Hum. Psychopharmacol. 2010; 25:193–200. [PubMed: 20373470]

Hugon J, Hugon F, Esclaire F, Lesort M, Diop AG. The presence of calbindin in rat cortical neurons protects in vitro from oxydative stress. Brain Res. 1996; 707:288–292. [PubMed: 8919307]

Huntington Study Group HART Investigators. A randomized, double-blind, placebo-controlled trial of pridopidine in Huntington's disease. Mov. Disord. 2013; 28:1407–1415. [PubMed: 23450660]

Hyrskyluoto A, Pulli I, Törnqvist K, Ho TH, Korhonen L, Lindholm D. Sigma-1 receptor agonist PRE084 is protective against mutant huntingtin-induced cell degeneration: involvement of calpastatin and the NF-κB pathway. Cell Death Dis. 2013; 4:e646. [PubMed: 23703391]

Jardin I, López JJ, Berna-Erro A, Salido GM, Rosado JA. Homer proteins in Ca^{2+} entry. IUBMB Life. 2013; 65:497–504. [PubMed: 23554128]

Jiang M, Chen G. High Ca^{2+}-phosphate transfection efficiency in low-density neuronal cultures. Nat. Protoc. 2006; 1:695–700. [PubMed: 17406298]

Kiyama H, Seto-Ohshima A, Emson PC. Calbindin D28K as a marker for the degeneration of the striatonigral pathway in Huntington's disease. Brain Res. 1990; 525:209–214. [PubMed: 2147568]

Kourrich S, Su TP, Fujimoto M, Bonci A. The sigma-1 receptor: roles in neuronal plasticity and disease. Trends Neurosci. 2012; 35:762–771. [PubMed: 23102998]

Langa F, Codony X, Tovar V, Lavado A, Giménez E, Cozar P, Cantero M, Dordal A, Hernández E, Pérez R, Monroy X, Zamanillo D, Guitart X, Montoliu L. Generation and phenotypic analysis of sigma receptor type I (σ1) knockout mice. Eur. J. Neurosci. 2003; 18:2188–2196. [PubMed: 14622179]

Li X, Chen W, Zhang L, Liu WB, Fei Z. Inhibition of store-operated calcium entry attenuates MPP(+)-induced oxidative stress via preservation of mitochondrial function in PC12 cells: involvement of Homer1a. PLoS One. 2013; 8:e83638. [PubMed: 24358303]

Li X, Hu Z, Liu L, Xie Y, Zhan Y, Zi X, Wang J, Wu L, Xia K, Tang B, Zhang R. A SIGMAR1 splice-site mutation causes distal hereditary motor neuropathy. Neurology. 2015; 84:2430–2437. [PubMed: 26078401]

Lundin A, Dietrichs E, Haghighi S, Göller ML, Heiberg A, Loutfi G, Widner H, Wiktorin K, Wiklund L, Svenningsson A, Sonesson C, Waters N, Waters S, Tedroff J. Efficacy and safety of the dopaminergic stabilizer pridopidine (ACR16) in patients with Huntington's disease. Clin. Neuropharmacol. 2010; 33:260–264. [PubMed: 20616707]

Luo P, Chen T, Zhao Y, Zhang L, Yang Y, Liu W, Li S, Rao W, Dai S, Yang J, Fei Z. Postsynaptic scaffold protein Homer 1a protects against traumatic brain injury via regulating group I metabotropic glutamate receptors. Cell Death Dis. 2014; 5:e1174. [PubMed: 24722299]

Luty AA, Kwok JB, Dobson-Stone C, Loy CT, Coupland KG, Karlström H, Sobow T, Tchorzewska J, Maruszak A, Barcikowska M, Panegyres PK, Zekanowski C, Brooks WS, Williams KL, Blair IP, Mather KA, Sachdev PS, Halliday GM, Schofield PR. Sigma nonopioid intracellular receptor 1 mutations cause frontotemporal lobar degeneration-motor neuron disease. Ann. Neurol. 2010; 68:639–649. [PubMed: 21031579]

MacDonald ME, Ambrose CM, Duyao MP, Myers RH, Lin C, Srinidhi L, Barnes G, Taylor SA, James M, Groot N, MacFarlane H, Jenkins B, Anderson MA, Wexler NS, Gusella JF. A novel gene containing a trinucleotide repeat that is expanded and unstable on Huntington's disease chromosomes. Cell. 1993; 72:971–983. [PubMed: 8458085]

Mao L, Yang L, Tang Q, Samdani S, Zhang G, Wang JQ. The scaffold protein Homer1b/c links metabotropic glutamate receptor 5 to extracellular signal-regulated protein kinase cascades in neurons. J. Neurosci. 2005; 25:2741–2752. [PubMed: 15758184]

Marrazzo A, Caraci F, Salinaro ET, Su TP, Copani A, Ronsisvalle G. Neuroprotective effects of sigma-1 receptor agonists against beta-amyloid-induced toxicity. Neuroreport. 2005; 16:1223–1226. [PubMed: 16012353]

Maruszak A, Safranow K, Gacia M, Gabryelewicz T, Słowik A, Styczyńska M, Pepłońska B, Golan MP, Żekanowski C, Barcikowska M. Sigma receptor type 1 gene variation in a group of Polish patients with Alzheimer's disease and mild cognitive impairment. Dement. Geriatr. Cogn. Disord. 2007; 23:432–438. [PubMed: 17457031]

Maurice T, Su TP. The pharmacology of sigma-1 receptors. Pharmacol. Ther. 2009; 124:195–206. [PubMed: 19619582]

Maurice T, Grégoire C, Espallergues J. Neuro (active) steroids actions at the neuromodulatory sigma 1 (σ 1) receptor: biochemical and physiological evidences, consequences in neuroprotection. Pharmacol. Biochem. Behav. 2006; 84:581–597. [PubMed: 16945406]

Mavlyutov TA, Epstein ML, Andersen KA, Ziskind-Conhaim L, Ruoho AE. The sigma-1 receptor is enriched in postsynaptic sites of C-terminals in mouse motoneurons. An anatomical and behavioral study. Neuroscience. 2010; 167:247–255. [PubMed: 20167253]

Meunier J, Ieni J, Maurice T. The anti-amnesic and neuroprotective effects of donepezil against amyloid beta25–35 peptide-induced toxicity in mice involve an interaction with the sigma1 receptor. Br. J. Pharmacol. 2006; 149:998–1012. [PubMed: 17057756]

Miller BR, Bezprozvanny I. Corticostriatal circuit dysfunction in Huntington's disease: intersection of glutamate, dopamine, and calcium. Future Neurol. 2010; 5:735–756. [PubMed: 21977007]

Milnerwood AJ, Raymond LA. Corticostriatal synaptic function in mouse models of Huntington's disease: early effects of huntingtin repeat length and protein load. J. Physiol. 2007; 585:817–831. [PubMed: 17947312]

Milnerwood AJ, Raymond LA. Early synaptic pathophysiology in neurodegeneration: insights from Huntington's disease. Trends Neurosci. 2010; 33:513–523. [PubMed: 20850189]

Mishina M, Ohyama M, Ishii K, Kitamura S, Kimura Y, Oda KI, Kawamura K, Sasaki T, Kobayashi S, Katayama Y, Ishiwata K. Low density of sigma1 receptors in early Alzheimer's disease. Ann. Nucl. Med. 2008; 22:151–156. [PubMed: 18498028]

Murmu RP, Li W, Holtmaat A, Li JY. Dendritic spine instability leads to progressive neocortical spine loss in a mouse model of Huntington's disease. J. Neurosci. 2013; 33:12997–13009. [PubMed: 23926255]

Myers RH, Vonsattel JP, Stevens TJ, Cupples LA, Richardson EP, Martin JB, Bird ED. Clinical and neuropathologic assessment of severity in Huntington's disease. Neurology. 1988; 38:341. [PubMed: 2964565]

Nguyen L, Lucke-Wold BP, Mookerjee SA, Cavendish JZ, Robson MJ, Scandinaro AL, Matsumoto RR. Role of sigma-1 receptors in neurodegenerative diseases. J. Pharmacol. Sci. 2015; 127:17–29. [PubMed: 25704014]

Nilsson M, Carlsson A, Markinhuhta KR, Sonesson C, Pettersson F, Gullme M, Carlsson ML. The dopaminergic stabiliser ACR16 counteracts the behavioural primitivization induced by the NMDA

receptor antagonist MK-801 in mice: implications for cognition. Prog. Neuro-Psychopharmacol. Biol. Psychiatry. 2004; 28:677–685.

Ortega-Roldan JL, Ossa F, Amin NT, Schnell JR. Solution NMR studies reveal the location of the second transmembrane domain of the human sigma-1 receptor. FEBS Lett. 2015; 589:659–665. [PubMed: 25647032]

Orth M, Schippling S, Schneider SA, Bhatia KP, Talelli P, Tabrizi SJ, Rothwell JC. Abnormal motor cortex plasticity in premanifest and very early manifest Huntington disease. J. Neurol. Neurosurg. Psychiatry. 2010; 81:267–270. [PubMed: 19828482]

Pal A, Fontanilla D, Gopalakrishnan A, Chae YK, Markley JL, Ruoho AE. The sigma-1 receptor protects against cellular oxidative stress and activates antioxidant response elements. Eur. J. Pharmacol. 2012; 682:12–20. [PubMed: 22381068]

Platt RJ, Chen S, Zhou Y, Yim MJ, Swiech L, Kempton HR, Dahlman JE, Parnas O, Eisenhaure TM, Jovanovic M, Graham DB, Jhunjhunwala S, Heidenreich M, Xavier RJ, Langer R, Anderson DG, Hacohen N, Regev A, Feng G, Sharp PA, Zhang F. CRISPR-Cas9 knockin mice for genome editing and cancer modeling. Cell. 2014; 159:440–455. [PubMed: 25263330]

Popugaeva E, Pchitskaya E, Speshilova A, Alexandrov S, Zhang H, Vlasova O, Bezprozvanny I. STIM2 protects hippocampal mushroom spines from amyloid synaptotoxicity. Mol. Neurodegener. 2015; 10:1–13. [PubMed: 25567526]

Ritchie ME, Phipson B, Wu D, Hu Y, Law CW, Shi W, Smyth GK. limma powers differential expression analyses for RNA-sequencing and microarray studies. Nucleic Acids Res. 2015; 43:e47. [PubMed: 25605792]

Roche KW, Tu JC, Petralia RS, Xiao B, Wenthold RJ, Worley PF. Homer 1b regulates the trafficking of group I metabotropic glutamate receptors. J. Biol. Chem. 1999; 274:25953–25957. [PubMed: 10464340]

Rodriguez A, Ehlenberger DB, Dickstein DL, Hof PR, Wearne SL. Automated three-dimensional detection and shape classification of dendritic spines from fluorescence microscopy images. PLoS One. 2008; 3:e1997. [PubMed: 18431482]

Rung JP, Rung E, Helgeson L, Johansson AM, Svensson K, Carlsson A, Carlsson ML. Effects of (−)-OSU6162 and ACR16 on motor activity in rats, indicating a unique mechanism of dopaminergic stabilization. J. Neural Transm. 2008; 115:899–908. [PubMed: 18351286]

Ruscher K, Shamloo M, Rickhag M, Ladunga I, Soriano L, Gisselsson L, Toresson H, Ruslim-Litrus L, Oksenberg D, Urfer R, Johansson BB, Nikolich K, Wieloch T. The sigma-1 receptor enhances brain plasticity and functional recovery after experimental stroke. Brain. 2011; 134:732–746. [PubMed: 21278085]

Ryskamp, DA.; Popugaeva, E.; Bezprozvanny, I. Calcium hypothesis of neurodegeneration: the case of Alzheimer's disease and Huntington's disease. In: Cummings, JL.; Pillai, JA., editors. Neurodegenerative Diseases: Unifying Principles. New York: Oxford University Press; 2016. p. 27-39.

Sahlholm K, Arhem P, Fuxe K, Marcellino D. The dopamine stabilizers ACR16 and (−)-OSU6162 display nanomolar affinities at the sigma-1 receptor. Mol. Psychiatry. 2013; 18:12–14. [PubMed: 22349783]

Sahlholm K, Sijbesma JW, Maas B, Kwizera C, Marcellino D, Ramakrishnan NK, Dierckx RA, Elsinga PH, van Waarde A. Pridopidine selectively occupies sigma-1 rather than dopamine D2 receptors at behaviorally active doses. Psychopharmacology. 2015; 232:3443–3453. [PubMed: 26159455]

Sanjana NE, Shalem O, Zhang F. Improved vectors and genome-wide libraries for CRISPR screening. Nat. Methods. 2014; 11:783–784. [PubMed: 25075903]

Schetz JA, Perez E, Liu R, Chen S, Lee I, Simpkins JW. A prototypical sigma-1 receptor antagonist protects against brain ischemia. Brain Res. 2007; 1181:1–9. [PubMed: 17919467]

Schippling S, Schneider SA, Bhatia KP, Münchau A, Rothwell JC, Tabrizi SJ, Orth M. Abnormal motor cortex excitability in preclinical and very early Huntington's disease. Biol. Psychiatry. 2009; 65:959–965. [PubMed: 19200948]

Schmidt HR, Zheng S, Gurpinar E, Koehl A, Manglik A, Kruse AC. Crystal structure of the human sigma1 receptor. Nature. 2016; 532:527–530. [PubMed: 27042935]

Shiraishi-Yamaguchi Y, Furuichi T. The Homer family proteins. Genome Biol. 2007; 8:206. [PubMed: 17316461]

Shoulson I, Fahn S. Huntington disease clinical care and evaluation. Neurology. 1979; 29:1–3. [PubMed: 154626]

Slow EJ, van Raamsdonk J, Rogers D, Coleman SH, Graham RK, Deng Y, Oh R, Bissada N, Hossain SM, Yang YZ, Li XJ, Simpson EM, Gutekunst CA, Leavitt BR, Hayden MR. Selective striatal neuronal loss in a YAC128 mouse model of Huntington disease. Hum. Mol. Genet. 2003; 12:1555–1567. [PubMed: 12812983]

Smith SB, Duplantier J, Dun Y, Mysona B, Roon P, Martin PM, Ganapathy V. In vivo protection against retinal neurodegeneration by sigma receptor 1 ligand (+)-pentazocine. Invest. Ophthalmol. Vis. Sci. 2008; 49:4154–4161. [PubMed: 18469181]

Squitieri F, Di Pardo A, Favellato M, Amico E, Maglione V, Frati L. Pridopidine, a dopamine stabilizer, improves motor performance and shows neuroprotective effects in Huntington disease R6/2 mouse model. J. Cell. Mol. Med. 2015; 11:2540–2548.

Srivats S, Balasuriya D, Pasche M, Vistal G, Edwardson JM, Taylor CW, Murrell-Lagnado RD. Sigma1 receptors inhibit store-operated Ca^{2+} entry by attenuating coupling of STIM1 to Orai1. J. Cell Biol. 2016; 213:65–79. [PubMed: 27069021]

Su TP, Hayashi T, Maurice T, Buch S, Ruoho AE. The sigma-1 receptor chaperone as an inter-organelle signaling modulator. Trends Pharmacol. Sci. 2010; 31:557–566. [PubMed: 20869780]

Sun S, Zhang H, Liu J, Popugaeva E, Xu NJ, Feske S, White CL, Bezprozvanny I. Reduced synaptic STIM2 expression and impaired store-operated calcium entry cause destabilization of mature spines in mutant presenilin mice. Neuron. 2014; 82:79–93. [PubMed: 24698269]

Tadokoro S, Tachibana T, Imanaka T, Nishida W, Sobue K. Involvement of unique leucine-zipper motif of PSD-Zip45 (Homer 1c/vesl-1 L) in group 1 metabotropic glutamate receptor clustering. Proc. Natl. Acad. Sci. U. S. A. 1999; 96:13801–13806. [PubMed: 10570153]

Takebayashi M, Hayashi T, Su T. A perspective on the new mechanism of antidepressants: neuritogenesis through sigma-1 receptors. Pharmacopsychiatry. 2004; 37:S208–S213. [PubMed: 15547787]

Tang TS, Tu H, Chan EY, Maximov A, Wang Z, Wellington CL, Hayden MR, Bezprozvanny I. Huntingtin and huntingtin-associated protein 1 influence neuronal calcium signaling mediated by inositol-(1,4,5) triphosphate receptor type 1. Neuron. 2003; 39:227–239. [PubMed: 12873381]

Tang TS, Slow E, Lupu V, Stavrovskaya IG, Sugimori M, Llinás R, Kristal BS, Hayden MR, Bezprozvanny I. Disturbed Ca^{2+} signaling and apoptosis of medium spiny neurons in Huntington's disease. Proc. Natl. Acad. Sci. U. S. A. 2005; 102:2602–2607. [PubMed: 15695335]

Tang TS, Guo C, Wang H, Chen X, Bezprozvanny I. Neuroprotective effects of inositol 1,4,5-trisphosphate receptor C-terminal fragment in a Huntington's disease mouse model. J. Neurosci. 2009; 29:1257–1266. [PubMed: 19193873]

Taylor CW, Genazzani AA, Morris SA. Expression of inositol trisphosphate receptors. Cell Calcium. 1999; 26:237–251. [PubMed: 10668562]

Tsai SY, Hayashi T, Harvey BK, Wang Y, Wu WW, Shen RF, Zhang Y, Becker KG, Hoffer BJ, Su TP. Sigma-1 receptors regulate hippocampal dendritic spine formation via a free radical-sensitive mechanism involving Rac1·GTP pathway. Proc. Natl. Acad. Sci. U. S. A. 2009; 106:22468–22473. [PubMed: 20018732]

Tsai SY, Rothman RK, Su TP. Insights into the sigma-1 receptor chaperone's cellular functions: a microarray report. Synapse. 2012; 66:42–51. [PubMed: 21905129]

Tsai SYA, Pokrass MJ, Klauer NR, Nohara H, Su TP. Sigma-1 receptor regulates Tau phosphorylation and axon extension by shaping p35 turnover via myristic acid. Proc. Natl. Acad. Sci. U. S. A. 2015; 112:674–6747.

Tu JC, Xiao B, Yuan JP, Lanahan AA, Leoffert K, Li M, Linden DJ, Worley PF. Homer binds a novel proline-rich motif and links group 1 metabotropic glutamate receptors with IP3 receptors. Neuron. 1998; 21:717–726. [PubMed: 9808459]

Uchida N, Ujike H, Tanaka Y, Sakai A, Yamamoto M, Fujisawa Y, Kanzaki A, Kuroda S. A variant of the sigma receptor type-1 gene is a protective factor for Alzheimer disease. Am. J. Geriatr. Psychiatry. 2005; 13:1062–1066. [PubMed: 16319298]

Villard V, Espallergues J, Keller E, Alkam T, Nitta A, Yamada K, Nabeshima T, Vamvakides A, Maurice T. Antiamnesic and neuroprotective effects of the aminotetrahydrofuran derivative ANAVEX1–41 against amyloid beta(25–35)-induced toxicity in mice. Neuropsychopharmacology. 2009; 34:1552–1566. [PubMed: 19052542]

Vonsattel JP, DiFiglia M. Huntington disease. J. Neuropathol. Exp. Neurol. 1998; 57:369–384. [PubMed: 9596408]

Wang J, Shanmugam A, Markand S, Zorrilla E, Ganapathy V, Smith SB. Sigma 1 receptor regulates the oxidative stress response in primary retinal Muller glial cells via NRF2 signaling and system xc(−), the Na(+)-independent glutamate-cystine exchanger. Free Radic. Biol. Med. 2015a; 86:25–36. [PubMed: 25920363]

Wang Y, Rao W, Zhang C, Liu M, Han F, Yao L, Han H, Luo P, Su N, Fei Z. Scaffolding protein Homer1a protects against NMDA-induced neuronal injury. Cell Death Dis. 2015b; 6:e1843. [PubMed: 26247728]

Worley PF, Zeng W, Huang G, Kim JY, Shin DM, Kim MS, Yuan JP, Kiselyov K, Muallem S. Homer proteins in Ca^{2+} signaling by excitable and non-excitable cells. Cell Calcium. 2007; 42:363–371. [PubMed: 17618683]

Wu J, Ryskamp DA, Liang X, Egorova P, Zakharova O, Hung G, Bezprozvanny I. Enhanced store-operated calcium entry leads to striatal synaptic loss in a Huntington's disease mouse model. J. Neurosci. 2016; 36:125–141. [PubMed: 26740655]

Wu J, Shih HP, Vigont V, Hrdlicka L, Diggins L, Singh C, Mahoney M, Chesworth R, Shapiro G, Zimina O, Chen X, Wu Q, Glushankova L, Ahlijanian M, Koenig G, Mozhayeva GN, Kaznacheyeva E, Bezprozvanny I. Neuronal store-operated calcium entry pathway as a novel therapeutic target for Huntington's disease treatment. Chem. Biol. 2011; 18:777–793. [PubMed: 21700213]

Wu Z, Bowen WD. Role of sigma-1 receptor C-terminal segment in inositol 1,4,5-trisphosphate receptor activation: constitutive enhancement of calcium signaling in MCF-7 tumor cells. J. Biol. Chem. 2008; 283:28198–28215. [PubMed: 18539593]

Yamada T, McGeer PL, Baimbridge KG, McGeer EG. Relative sparing in Parkinson's disease of substantia nigra dopamine neurons containing calbindin-D28K. Brain Res. 1990; 526:303–307. [PubMed: 2257487]

de Yebenes JG, Landwehrmeyer B, Squitieri F, Reilmann R, Rosser A, Barker RA, Saft C, Magnet MK, Sword A, Rembratt Å, Tedroff J. MermaiHD study investigators. Pridopidine for the treatment of motor function in patients with Huntington's disease (MermaiHD): a phase 3, randomised, double-blind, placebo-controlled trial. Lancet Neurol. 2011; 10:1049–1057. [PubMed: 22071279]

Yenari MA, Minami M, Sun GH, Meier TJ, Kunis DM, McLaughlin JR, Ho DY, Sapolsky RM, Steinberg GK. Calbindin d28k overexpression protects striatal neurons from transient focal cerebral ischemia. Stroke. 2001; 32:1028–1035. [PubMed: 11283407]

Zeng X, Pan ZG, Shao Y, Wu XN, Liu SX, Li NL, Wang WM. SKF-96365 attenuates toxin-induced neuronal injury through opposite regulatory effects on Homer1a and Homer1b/c in cultured rat mesencephalic cells. Neurosci. Lett. 2013; 543:183–188. [PubMed: 23567742]

Zhang H, Wu L, Pchitskaya E, Zakharova O, Saito T, Saido T, Bezprozvanny I. Neuronal store-operated calcium entry and mushroom spine loss in amyloid precursor protein knock-in mouse model of Alzheimer's disease. J. Neurosci. 2015; 35:13275–13286. [PubMed: 26424877]

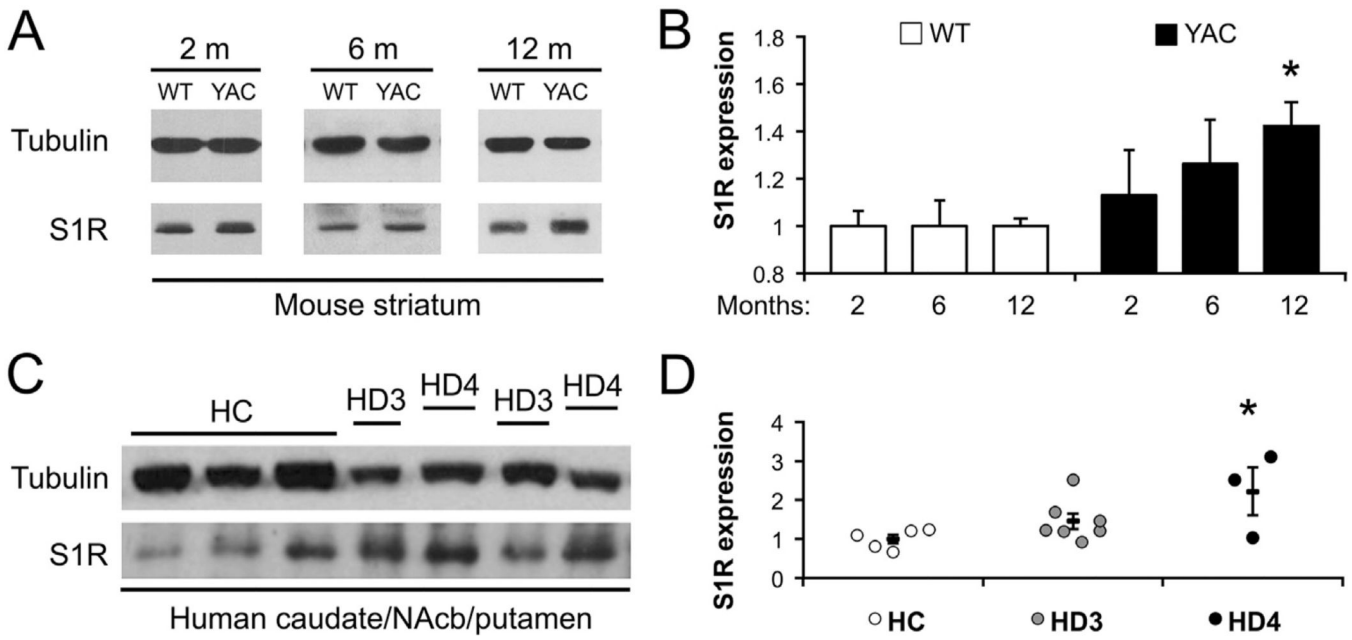

Fig. 1.

Age-dependent striatal S1R upregulation in HD. (A–B) S1R protein expression in striatal samples from WT and YAC128 mice at 2, 6 and 12 months of age. Tubulin was used as a loading control. Results were normalized to the S1R expression level in the WT condition for each age and are shown as mean ± S.E. WT and YAC128 were compared at each age using a Sidak post-test. (C–D) S1R protein expression in samples from human brain. HC = healthy controls. HD3 = moderate HD. HD4 = severe HD. Results were normalized to the HC condition. HD conditions were compared to the HC condition using a Dunnett's post-test. *$p < 0.05$.

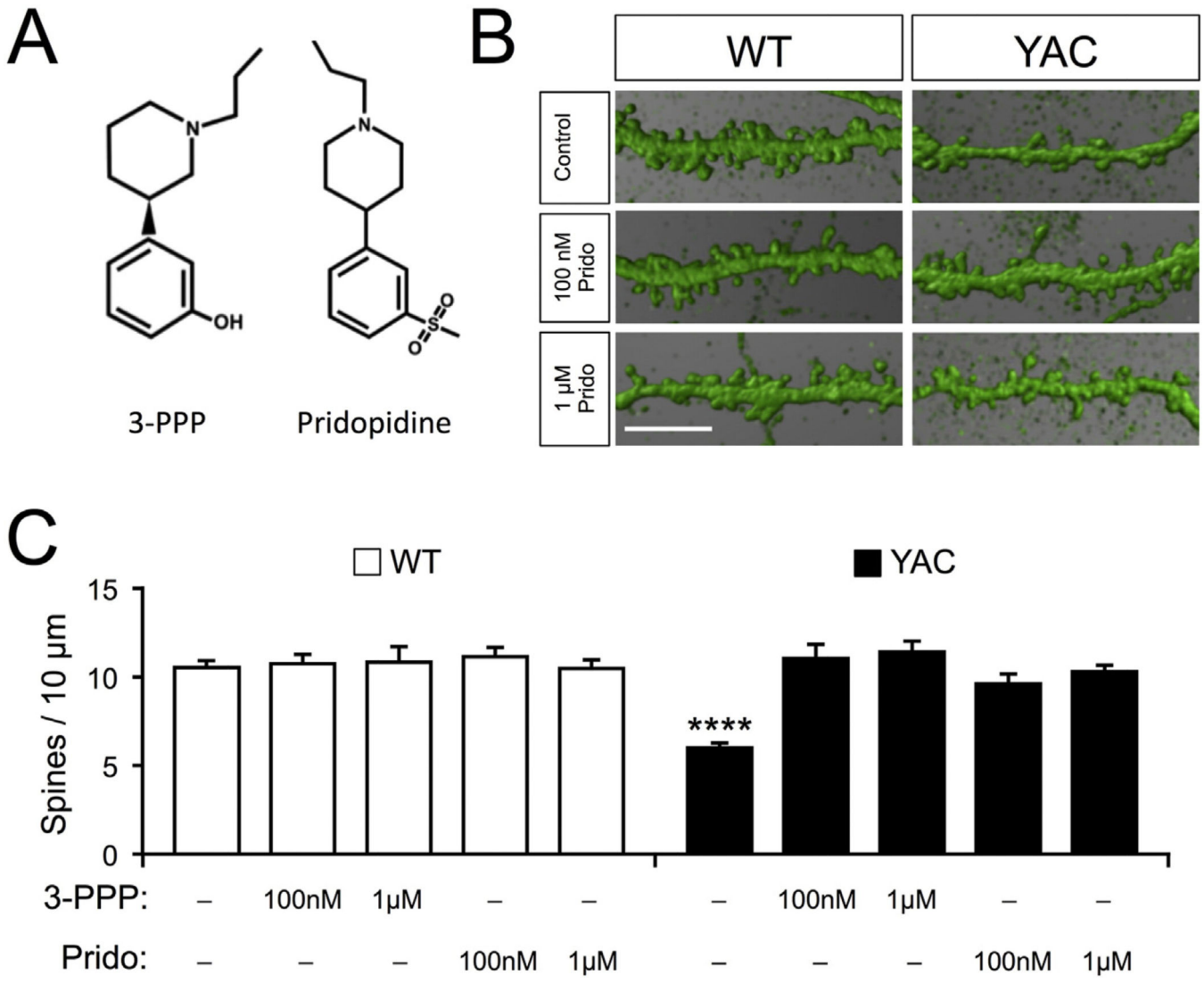

Fig. 2.

Pridopidine and 3-PPP prevent loss of MSN spines in aged corticostriatal co-cultures from YAC128 mice. (A) Chemical structures of 3-PPP and pridopidine adapted from Sahlholm et al. (2013). (B) 3D reconstructions of MSN spines based on DARPP32 staining in WT and YAC128 corticostriatal co-cultures. Scale bar = 10 µm. (C) Quantitative summary of MSN spine density in corticostriatal co-cultures from WT and YAC128 mice treated with vehicle, 3-PPP or pridopidine for 16 h starting on DIV21. Results are shown as mean ± S.E. All experimental conditions were compared to the WT control condition using a Dunnett's post-test. ****$p < 0.0001$.

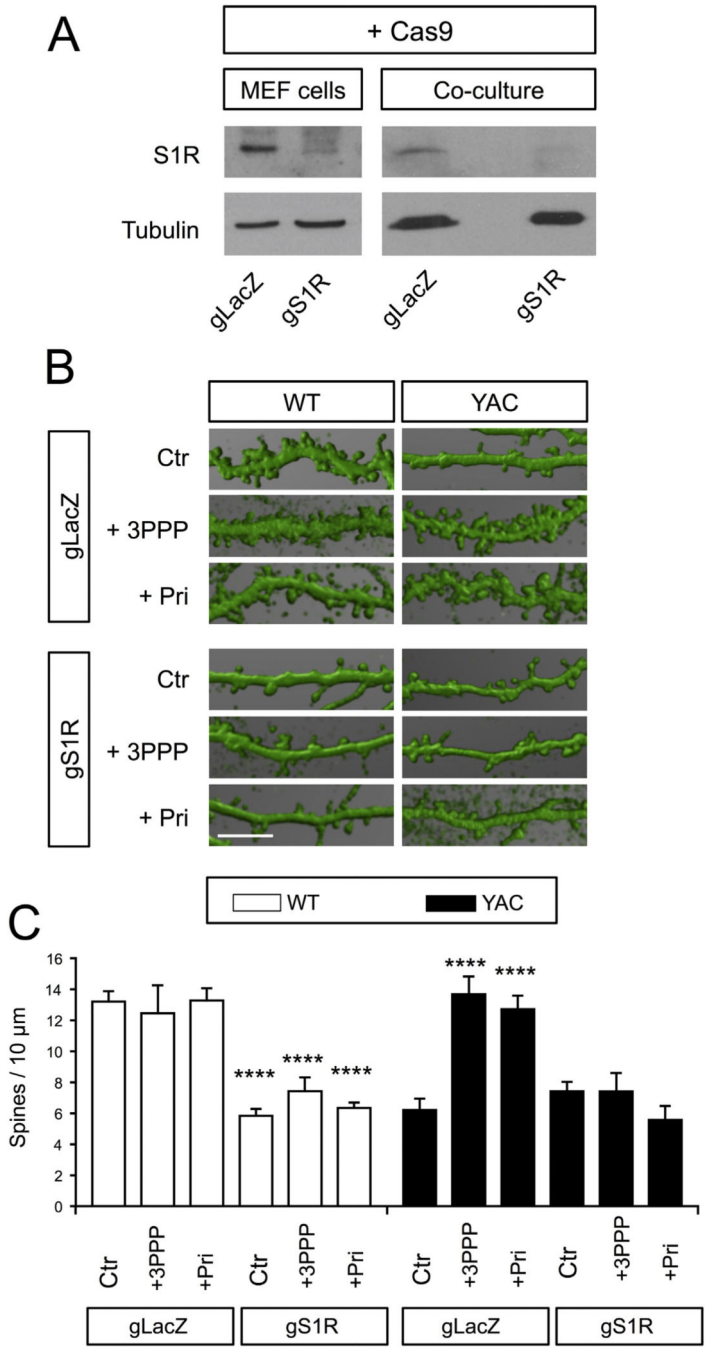

Fig. 3.

Knock out of S1R prevents rescue of MSN spines by pridopidine and 3-PPP. (A) Western blot analysis of S1R expression in MEF cells transfected with Cas9 and gS1R or gLacZ plasmids. Transfected cells were selected with 5 µg/ml blasticidin and 10 µg/ml puromycin. Tubulin was used as a loading control. Corticostriatal co-cultures were transfected with lenti-Cas9 and lenti-gS1R (gS1R) or lenti-Cas9 and lenti-gLacZ (gLacZ) on DIV7 and S1R protein expression was analyzed on DIV22. (B) WT and YAC128 corticostriatal co-cultures were infected with lenti-Cas9 and lenti-gS1R (gS1R) or lenti-Cas9 and lenti-gLacZ (gLacZ)

on DIV7. Cultures were treated for 16 h with the vehicle, 100 nM 3-PPP or 100 nM pridopidine starting on DIV21. The cultures were fixed at DIV22 and stained for DARPP32. 3D reconstructions of spines are shown. Scale bar = 10 μm. (C) The spine density for each experimental condition is shown as mean ± S.E. Statistical comparisons were made to the gLacZ control condition for WT and YAC128 cultures using Dunnett's post-test. ****$p < 0.0001$.

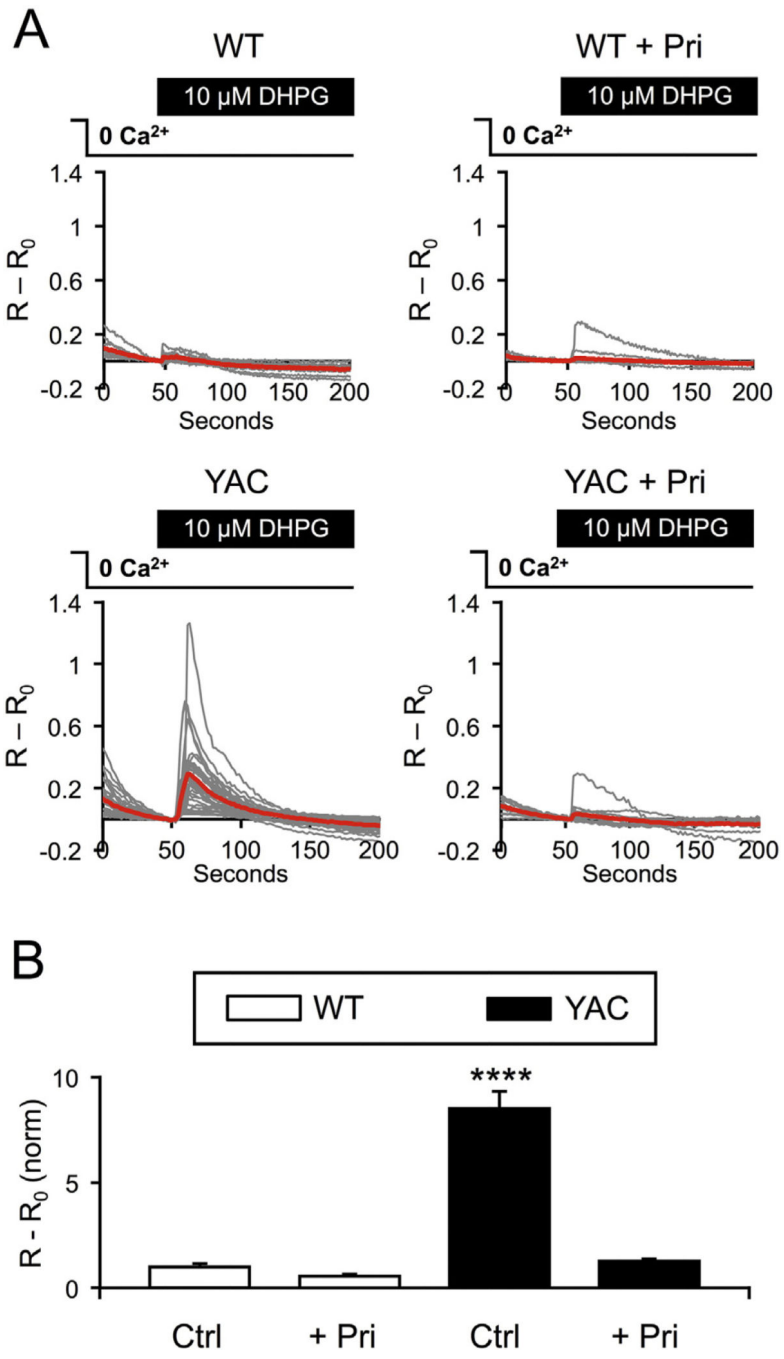

Fig. 4.

Pridopidine normalizes $InsP_3R1$-dependent calcium release in YAC128 MSNs. (A) Fura-2 340/380 fluorescence ratio traces are shown for WT and YAC128 MSN cell bodies (red = averaged trace, gray = individual traces). External calcium was removed and 10 μM DHPG was applied after 60 s. Traces are shown for control cultures (left) and for cultures treated with 1 μM pridopidine for 16–24 h prior to starting the experiment (right). (B) The mean amplitudes of DHPG-evoked responses were normalized to the WT control condition and

are shown as mean ± S.E. Comparisons were made to the WT control condition. ****$p <$ 0.0001.

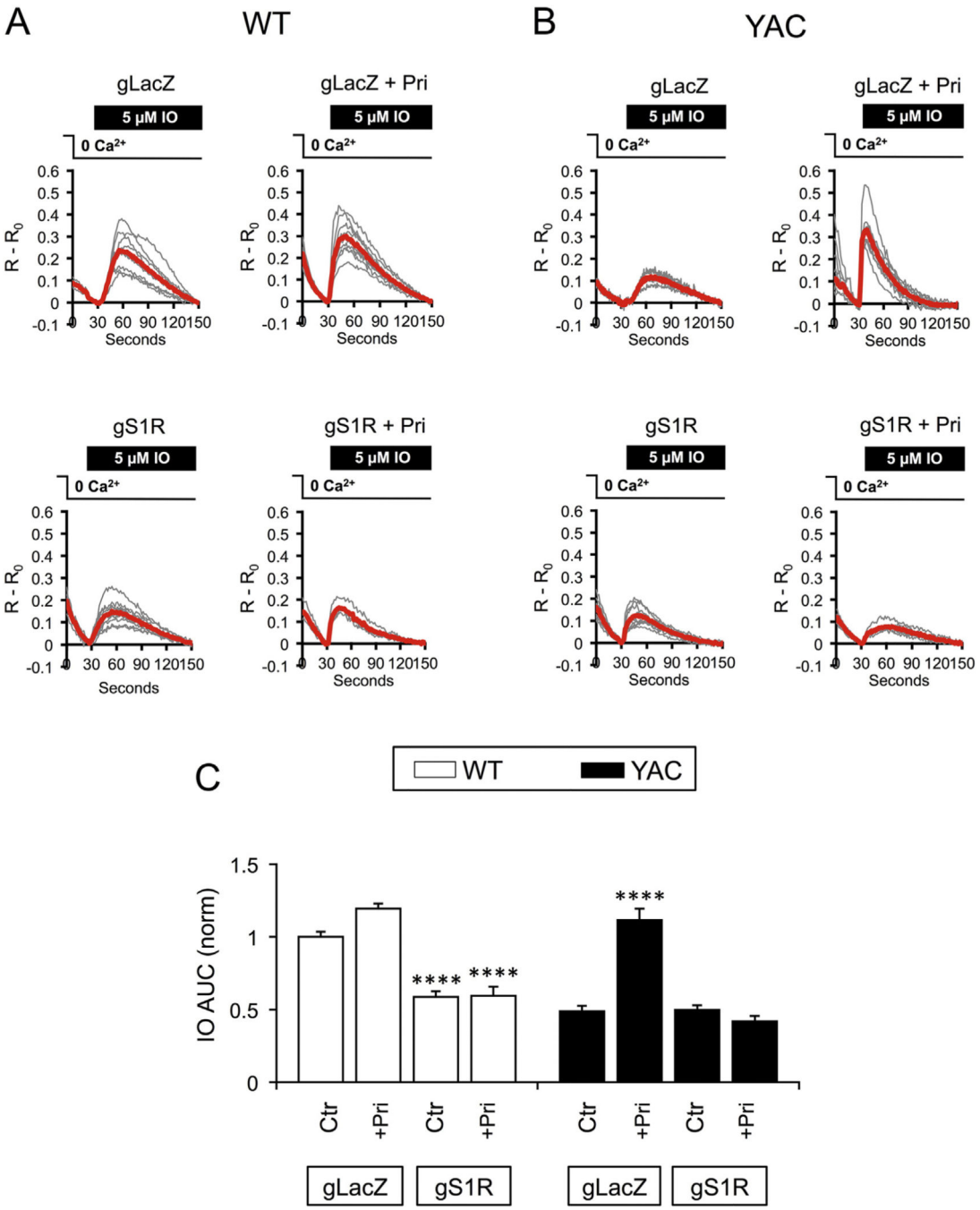

Fig. 5.

Pridopidine normalizes YAC128 MSN ER Ca^{2+} levels. (A) Fura-2 340/380 fluorescence ratio traces are shown for WT and YAC128 MSN cell bodies (red = averaged trace, gray = individual traces). 30 s after calcium was removed from the bath solution, cultures were treated with 5 μM ionomycin (IO) to release Ca^{2+} from the ER. Calcium imaging was performed on DIV13–15. Cultures were co-infected on DIV7 with lenti-Cas9 and lenti-gLacZ (gLacZ; top) or lenti-Cas9 and lenti-gS1R (gS1R; bottom) viruses. Traces are shown for cultures treated with 1 μM pridopidine for 16–24 h prior to starting the experiment (right

for each genotype) and vehicle-treated controls (left for each genotype). (B) The average size of the IO-sensitive Ca^{2+} pool was calculated by integrating the area under Fura-2 traces. The results were normalized to the IO pool size in WT control cultures and are shown as mean ± S.E. Statistical comparisons were made to the gLacZ control condition for WT and YAC128 cultures using Dunnett's post-test. ****$p < 0.0001$.

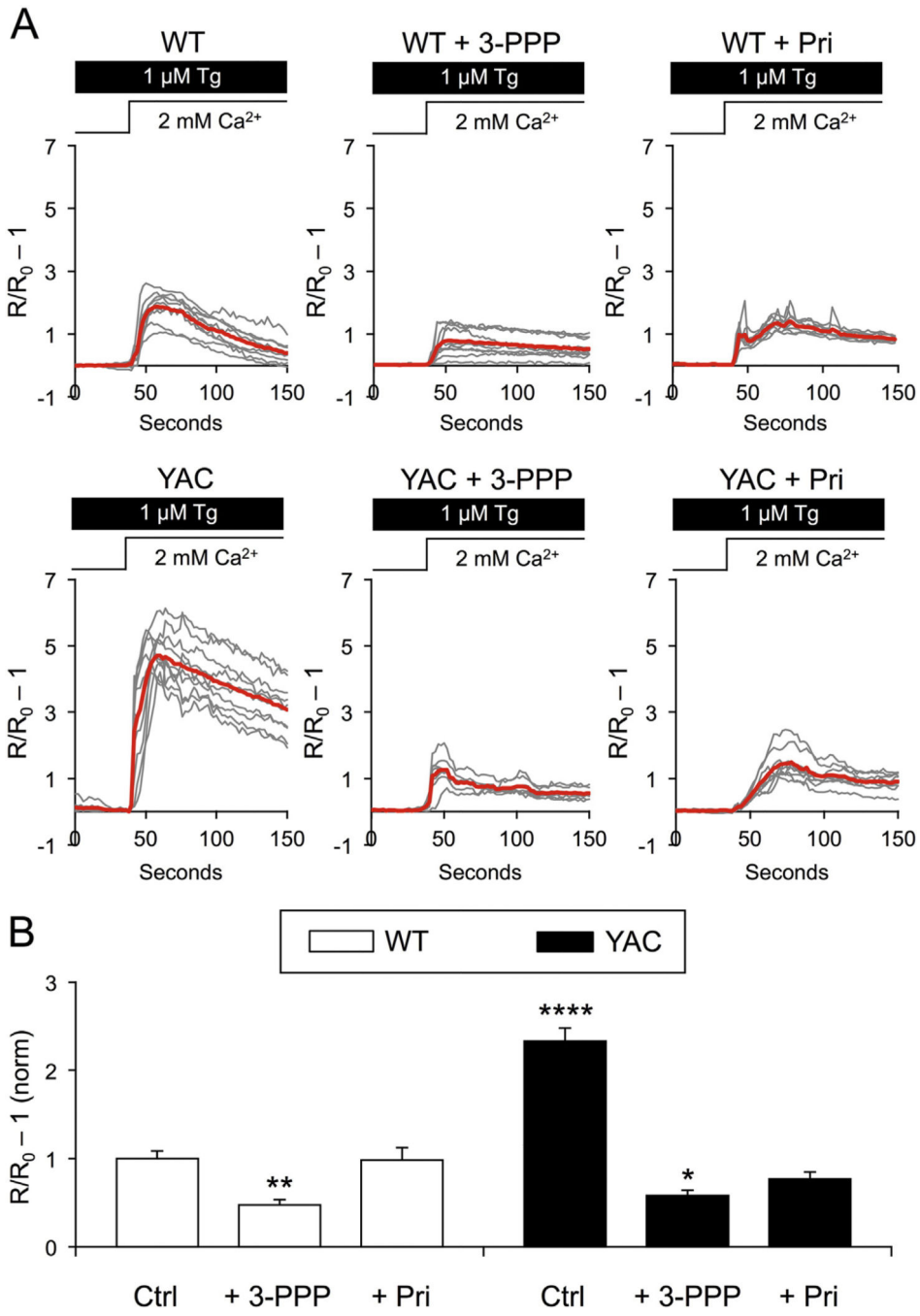

Fig. 6.

3-PPP and pridopidine normalize YAC128 MSN spine nSOC. (A) GCaMP5G fluorescence traces in WT and YAC128 MSN spines during the Ca^{2+} "add-back" protocol for SOC measurement (red = averaged trace, gray = individual traces). SERCA pump activity was blocked with 1 μM thapsigargin (Tg) to deplete ER Ca^{2+} in the absence of external Ca^{2+} for 5 min prior to adding 2 mM Ca^{2+} back to the ACSF. Cultures were treated with the vehicle, 1 μM 3-PPP or 1 μM Pridopidine for 16–24 h starting on DIV14. (B) The average peak of spine SOC was quantified. Results were normalized to WT control cultures and are shown as

mean ± S.E. Comparisons to the WT control condition were made with Tukey's post-test. *$p < 0.05$. **$p < 0.01$. ****$p < 0.0001$.

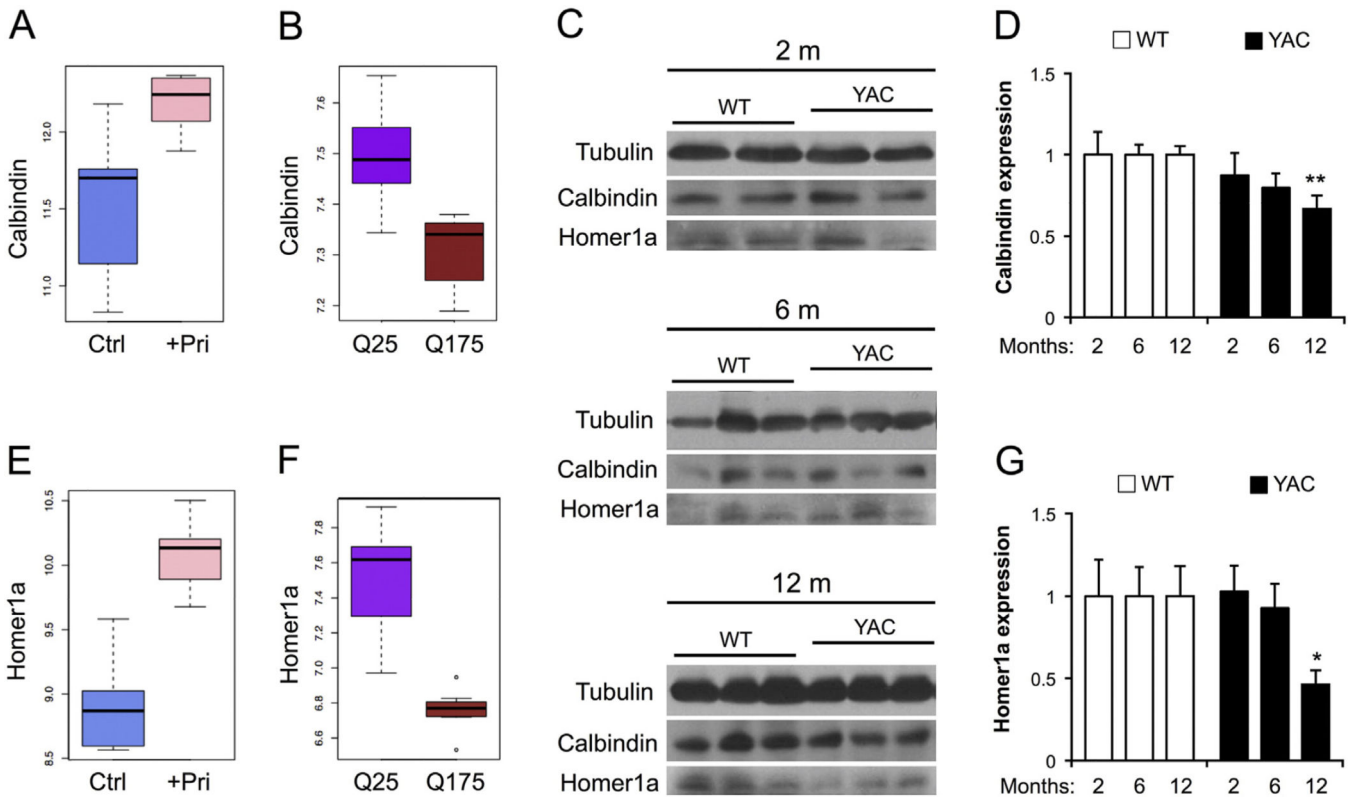

Fig. 7.

Key calcium regulating genes, Calb1 and homer1a, are significantly downregulated in HD mouse striatum and are both significantly upregulated by pridopidine treatment. (A) Striatal gene expression of calbindin (Calb1) is increased after chronic treatment with pridopidine in healthy rats ($p = 4.2E{-}3$; adj. $p = 0.4$). (B) Striatal gene expression of Calb1 is decreased in a mouse HD model carrying 175 CAG repeats (Q175) when compared with controls carrying 25 CAG repeats (Q25) ($p = 3.3E{-}4$; adj. $p = 4.2E{-}3$). (C) Calbindin protein in striatal lysates from WT and YAC128 was analyzed at 2, 6, and 12 months by Western blotting. Tubulin was used as a loading control. The same membranes used for analysis of calbindin expression were stripped and re-blotted for Homer 1a. (D) Calbindin expression was normalized to the calbindin expression level in the WT condition for each age and is shown as mean ± S.E. (E) Gene expression of homer1a is increased in rat striatum following chronic pridopidine treatment in healthy rats ($p = 7.7E{-}06$; adj. $p = 0.02$). (F) Gene expression of the homer1a gene is decreased in the Q175 mouse model as compared to the Q25 control ($p = 9.4E{-}06$; adj. $p = 2.5E{-}4$). (C, G) Homer1a protein in striatal lysates from WT and YAC128 was analyzed at 2, 6, and 12 months by Western blotting. Homer1a expression was normalized to the Homer1a expression level in the WT condition for each age and is shown as mean ± S.E. For analysis of Western blots comparisons were made to the age-matched WT samples. $*p < 0.05$, $**p < 0.01$.